DIGITAL DOPPLER PROCESSING USING WALSH AND QUANTIZED FOURIER TRANSFORMS

J. L. Ekstrom

Johns Hopkins University

Prepared for:

Naval Plant Representative Office

November 1974

PLEASE FOLD BACK IF NOT NEEDED FOR BIBLIOGRAPHIC PURPOSES

REPORT DOCUMENTATION PAGE

1. REPORT NUMBER	2. GOVT ACCESSION NO	3. RECIPIENT'S CATALOG NUMBER
APL/JHU TG 1265		AD-A026 116

4. TITLE (and Subtitle)

DIGITAL DOPPLER PROCESSING USING WALSH AND QUANTIZED FOURIER TRANSFORMS

5. TYPE OF REPORT & PERIOD COVERED

Technical Report

6. PERFORMING ORG. REPORT NUMBER

7. AUTHOR(s)

J. L. Ekstrom

8. CONTRACT OR GRANT NUMBER(s)

N00017-72-C-4401

9. PERFORMING ORGANIZATION NAME & ADDRESS

The Johns Hopkins University Applied Physics Laboratory
8621 Georgia Ave.
Silver Spring, Md. 20910

10. PROGRAM ELEMENT, PROJECT, TASK AREA & WORK UNIT NUMBERS

Task A64

11. CONTROLLING OFFICE NAME & ADDRESS

Naval Plant Representative Office
8621 Georgia Ave.
Silver Spring, Md. 20910

12. REPORT DATE

November 1974

13. NUMBER OF PAGES

~~86 (4 blank)~~ 79

14. MONITORING AGENCY NAME & ADDRESS

Naval Plant Representative Office
8621 Georgia Ave.
Silver Spring, Md. 20910

15. SECURITY CLASS (of this report)

Unclassified

15a. DECLASSIFICATION/DOWNGRADING SCHEDULE

NA

16. DISTRIBUTION STATEMENT (of this Report)

Approved for public release; distribution unlimited.

17. DISTRIBUTION STATEMENT (of the abstract entered in Block 20, if different from Report)

18. SUPPLEMENTARY NOTES

19. KEY WORDS (Continue on reverse side if necessary and identify by block number)

Doppler filter synthesis
Walsh and Fourier transforms
Digital doppler processing
Walsh transforms
Quantized Fourier transforms

20. ABSTRACT (Continue on reverse side if necessary and identify by block number)

The use of Walsh and Fourier transforms to synthesize banks of contiguous doppler filters is examined in considerable detail for 32-point transforms and in less detail for 256-point transforms. It is found that the use of Walsh or hard-limited Fourier transforms results in the introduction of numerous large spurious sidelobes or artifacts in the filter responses, and that these artifacts are essentially unaffected by input signal amplitude tapering. It is shown how the artifacts may be reduced in size and number by increasing the number of quantization levels in the Fourier transform.

DD FORM 1 JAN 73 1473

APL/JHU
TG 1265
NOVEMBER 1974
Copy No.

Technical Memorandum

DIGITAL DOPPLER PROCESSING USING WALSH AND QUANTIZED FOURIER TRANSFORMS

by J. L. EKSTROM

THE JOHNS HOPKINS UNIVERSITY • APPLIED PHYSICS LABORATORY
8621 Georgia Avenue ◦ Silver Spring, Maryland ◦ 20910
Operating under Contract N00017-72-C-4401 with the Department of the Navy

1.

THE JOHNS HOPKINS UNIVERSITY
APPLIED PHYSICS LABORATORY
SILVER SPRING MARYLAND

CONTENTS

Preceding page blank

ILLUSTRATIONS

ILLUSTRATIONS (cont'd)

ILLUSTRATIONS (cont'd)

ILLUSTRATIONS (cont'd)

1.0 INTRODUCTION AND SUMMARY

For practical reasons involving available signal bandwidths at microwave frequencies, the process of radar target velocity estimation generally involves measuring the frequency of a time-limited sinusoidal carrier signal in the presence of additive noise (and possibly other target signals) and using the doppler equation to convert frequency to velocity. (Target acceleration is assumed to be zero during the radar observation interval.)

The frequency measurement process generally involves "matching" the received signal waveform with a finite number of stored or reference signal waveforms having different carrier frequencies in order to see which one best matches the received signal. The matching process generally involves either multiplication and integration in the case of analog signals, or multiplication, sampling, and summation in the case of sampled waveforms.

Although sinusoidal reference signals have been used very successfully for many years, and may be expected intuitively to provide the best kind of matching to sinusoidal radar returns, they are quite costly to implement in a digital signal processing system. The question naturally arises as to whether some other type or types of reference signals might cost much less and provide only slightly inferior results.

From the very large class of possible substitute reference waveforms, three candidates have been chosen for analysis:

1. Walsh waveforms,
2. Hard-limited circular waveforms, and
3. Quantized circular waveforms.

The use of hard-limited circular waveforms in digital systems permits the operation of multiplication to be replaced by signed addition, a much simpler and cheaper operation. However, square waves do not "look" much like sinusoids, and so the frequency estimation process might be degraded. The use of quantized sinusoidal reference waveforms would be expected to produce results and costs somewhere (depending on the number of quantization levels) between those of the hard-limited case and the conventional sinusoidal case.

The use of Walsh reference waveforms is investigated here in some detail for a number of reasons. First, they are binary valued like square waves, so that multiplication can again be replaced by signed addition. Second, in recent years an increased interest has been shown in the application of Walsh function waveforms to a wide variety of tasks (see the Bibliography and Refs. 1 through 4), so their applicability to radar signal processing tasks would seem to be worthy of study. Third, a limited amount of work in this area has already been accomplished, Refs. 3 and 4; the results suggest that Walsh functions are inferior to circular functions as far as the frequency estimation problem is concerned, but not enough data are presented to answer such basic questions as: How do the clutter rejection capabilities of such filters compare to those obtainable via Fourier processing using quantized circular functions? Does the use of Walsh functions result

---

Ref. 1. H. F. Harmuth, Transmission of Information by Orthogonal Functions, Springer-Verlag, First Ed. 1969, Second Ed. 1972.

Ref. 2. N. M. Blachman, "Sinusoids versus Walsh Functions," Proc. IEEE, Vol. 62, March 1974, pp. 346-354.

Ref. 3. J. Salzman, Discrete Transform Methods in Adaptive Radar Detection, M. S. Thesis, UCLA, 1973.

Ref. 4. J. Pearl and J. Salzman, "Comparison of Fourier and Walsh Transforms in Radar Signal Processing," Proc. 1973 Symp. on the Applications of Walsh Functions.

in the introduction of spurious responses which could complicate the multiple target resolution problem?

The paragraphs above have been intentionally written in a rather general fashion to provide an easily understood introduction to the work reported in this report. By way of a more specific introduction, this report describes the results obtained from a rather detailed investigation of the comparative performance of Discrete Walsh Transforms (DWT's) and Discrete Fourier Transforms (DFT's) in the task of synthesizing a doppler filter bank using digital baseband quadrature processing. A comparison is made of the filter response curves obtained by using the DWT with those obtainable from the DFT using various levels of quantization of the sine and cosine reference signals. The use of quantized reference signals in the DFT has received some attention in the past (Refs. 5 and 6), but our results are believed to contain considerably more detailed information than has heretofore been available. In certain cases they also illustrate the transition from pure Fourier to pure Walsh processing.

Both 32-point and 256-point transforms were investigated in this study – the former in great detail and the latter for those situations where the Walsh functions degenerate into square waves. For the 32-point transform it is shown that, from a spurious sidelobe number and amplitude point of view, the DWT is inferior to the DFT, even when the DFT uses hard-limited sines and cosines for the reference waveforms. The limited amount of 256-point transform data obtained fails to indicate that this

---

Ref. 5. D. W. Tufts, H. S. Hersey, and W. E. Mosier, "Effects of FFT Coefficient Quantization on Bin Frequency Response," Proc. IEEE, January 1972, pp. 146-147.

Ref. 6. D. W. Tufts, D. W. Rorabacher, and W. E. Mosier, "Designing Simple, Effective Digital Filters," IEEE Trans. Audio and Electroacoustics, Vol. AU-18, June 1970, pp. 142-158.

inferiority might be a function of the number of points in the transform, and so further study of the DWT for this particular application does not seem to be warranted.

Subsequent sections of this report deal with the various aspects of the analyses undertaken; a detailed discussion of the results is presented in Section 4.

2.0 DESCRIPTION OF PROBLEM

Various workers (Refs. 7 and 8) have described two-dimensional signal processing filters capable of separating signals on both a doppler frequency and range basis. A very flexible technique for performing the doppler filtering part of the processing uses the baseband quadrature processing technique described by Nathanson (Ref. 9). This technique provides an estimate of incoming doppler frequency which is independent of the starting phase angle of the received waveform. Furthermore, both positive and negative dopplers may be separately distinguished; the only requirement imposed by the sampling process is that the magnitude of the doppler frequency must not exceed one-half the sampling frequency.

In the following sections, processing in a single dimension using the Nathanson scheme is considered for a variety of correlation waveforms. The results are valid in the strictest sense only along one of the principal axes of the two dimensional processor; at other points in the range doppler plane the sidelobe performance would probably be poorer.

The use of Fourier techniques to estimate the doppler frequency basically involves correlating the received waveform with stored reference waveforms that are sinusoidal or cosinusoidal in shape and have fixed frequencies separated by the reciprocal of the observation interval. The number of different reference waveform frequencies, and hence the number of filter outputs available, is equal

---

Ref. 7. R. A. Meyer, D. G. Grant, J. L. Queen, A Digital-Optical Hybrid Correlator, APL/JHU TG 1193A, September 1972.

Ref. 8. W. H. Zinger and R. F. Platte, personal communication.

Ref. 9. E. E. Nathanson, Radar Design Principles, Section 14.8, McGraw Hill, 1969.

to N, the number of points in the transform. The magnitude of any filter output is a measure of how close the input frequency is to the reference frequency uniquely associated with that particular filter, so that the frequency estimation process in its simplest form involves looking at the N filter outputs to determine which one is the largest. Of course, if the input frequency lies between two reference frequencies some interpolation may be needed to find the input frequency, since the input frequencies do not have to coincide exactly with any of the stored reference frequencies.

For a single input frequency, in the absence of additive noise, the frequency estimation process is unambiguous. However, the magnitude of the nth output, while reaching a maximum value at some input frequency f_n, has also unavoidably some (hopefully small) output at other frequencies not equal to f_n. This off-frequency response is quantified by the sidelobe levels of the filter response. If the sidelobe levels are everywhere quite small for every filter, there will be small chance that noise or other input signals will corrupt the unambiguous frequency estimation process; however, large sidelobes will greatly increase the chances for corruption.

The Fourier processor normally produces filter sidelobe levels that fall off with frequency according to the $(\frac{\sin f}{f})^2$ form typified by the power patterns of uniformly illuminated linear antenna apertures. The sidelobes can be reduced by weighting or tapering the input signal level as a function of time during the observation interval; the process is exactly analogous to aperture tapering in a linear array.

Although sinusoids are most commonly used as reference waveforms, the frequency estimation process can be performed using other types of waveforms, and the use of Walsh functions and quantized sinusoids as reference waveforms will be studied here. As mentioned in Section 1.0, these waveforms will be shown to produce generally inferior results from the sidelobe level point of view, and these sidelobe levels are minimally affected by input signal tapering.

3.0 MODEL DESCRIPTION AND METHOD OF ANALYSIS

Figure 1 is a simplified block diagram of one channel of the type of processor analyzed in this study. The baseband quadrature input signals are sinusoids of arbitrary starting phase ϕ and frequency f. The frequency f may be positive or negative, corresponding to approaching or receding targets, but its magnitude must not exceed half the sampling frequency f_s, and the input signals and correlation waveforms are assumed without loss of generality to have unit duration. The indicated sampling and summing operations in Fig. 1 are carried out within the unit time interval. At the end of this interval the sums are squared and added to yield the channel output, which will be independent of ϕ. A(t) is a data weighting window, which in this study has two forms. The first form is a unity level over the unit time interval; the second form is the Hamming (Ref. 10) weighting function given by:

$$A(t) = \frac{1}{2}\,[1 - 0.852 \cos 2\pi t],\ 0 \le t \le 1\ , \qquad (1)$$

which for nonquantized Fourier processing yields filter sidelobes that are all at least 40 dB below any filter mainlobe.

W_c and W_s are the quadrature correlation waveforms and are indexed by the parameter i, which, in addition to the values zero and N/2 (N being the number of points in the transform), may assume the values ±1, ±2, ----- $\pm (\frac{N}{2} - 1)$. The positive values of i correspond to filters "tuned" to input frequencies given by $f_0 = i$, while the negative values correspond to filters tuned to values of f_0 given by $f_0 = N + i$. For Fourier processing W_c and W_s will be given by

$$W_c(i,t) = [\cos(2\pi it)]_Q \qquad (2)$$

$$W_s(i,t) = [\sin(2\pi it)]_Q \qquad (3)$$

Ref. 10 R. B. Blackman and J. W. Tukey, The Measurement of Power Spectra, Dover Publications, 1959.

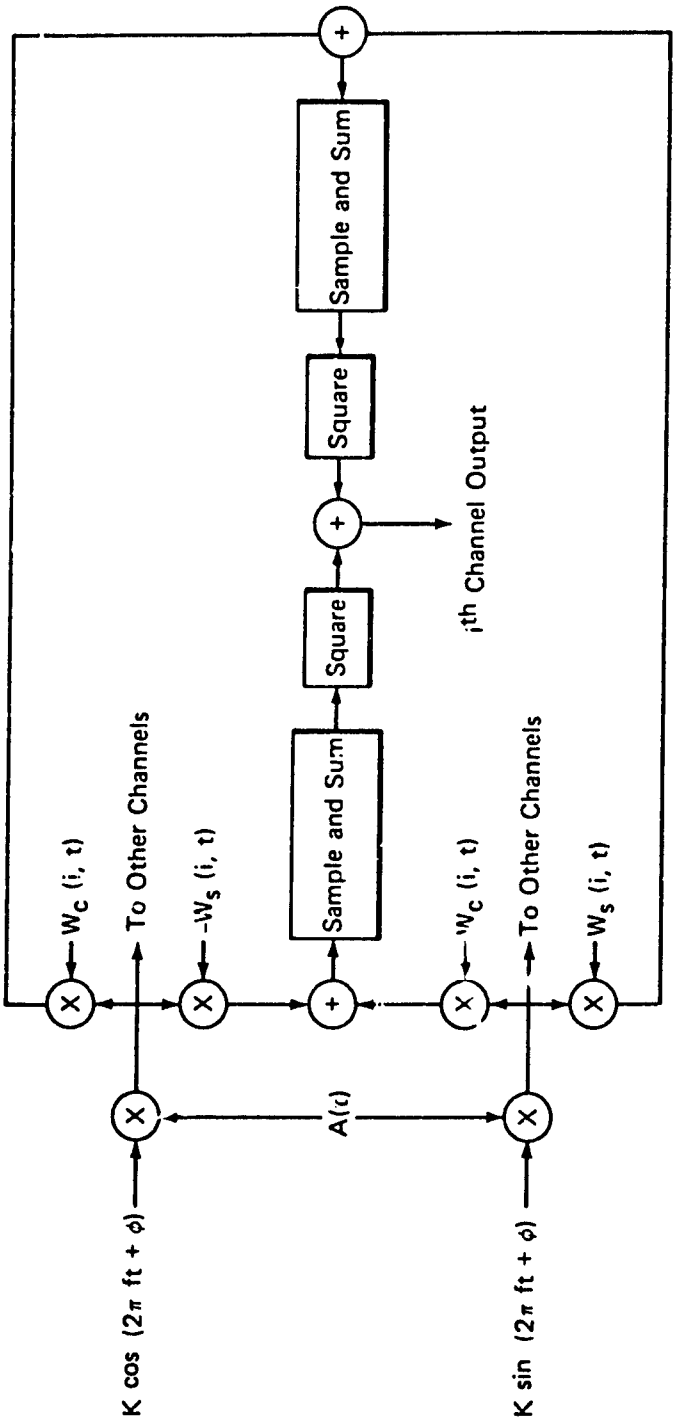

Fig. 1 Quadrature Channel Processor General Block Diagram for ith Channel

where the $[\ ]_Q$ bracket signifies that the values of the circular functions may be quantized to a number of levels. In the computer simulations used here, this means that the values are expressed as a sign bit together with some number of amplitude bits following the binary point, the exact representation being obtained by rounding rather than by truncating. Note that W_c and W_s may be zero for certain values of i and t, and that they are defined only at the sampling instants.

For Walsh processing W_c and W_s are not periodic, except when i is an integer power of two, in which case W_c and W_s are hard limited cosine and sine functions, respectively. For other values of i, the i denotes the "sequency" of the Walsh function, which is half the average number of zero crossings per unit interval, and is thus analogous to "frequency" in the Fourier case. Formally, W_c and W_s are defined by

$$W_c(i,t) = \mathrm{WAL}(2i,t) = \mathrm{CAL}(i,t), \text{ all } i \tag{4}$$

$$\begin{aligned} W_s(i,t) &= \mathrm{WAL}(2i-1,t) \\ &= \mathrm{SAL}(i,t), \ i > 0 \\ &= 0, \ i = 0 \\ &= -\mathrm{SAL}(-i,t), \ i < 0 \end{aligned} \tag{5}$$

where the WAL, CAL, and SAL functions are discussed and illustrated in Ref. 2, and in the Introduction chapter of the second edition of Ref. 1, with $t = 0$ in the latter reference corresponding to $\theta = -1/2$. Sampled values of the SAL and CAL waveforms are stored in the computer for use in the calculations, and several sets are given for a 32-point transform in Table 1, where "+" = +1 and "-" = -1. The square wave nature of the CAL and SAL functions for the case $i = 8$ can be easily discerned from the sample sequences in the second column of Table 1, and the interested reader may wish to compare the SAL and CAL sample sequences for $i = 3$ with the WAL(5,t) and WAL(6,t) waveform plots given in Fig. 1 of Ref. 2.

Table 1

Examples of Sampled CAL and SAL Functions

SAMPLE NO.	i = 3		i = 8		i = 15	
	CAL	SAL	CAL	SAL	CAL	SAL
1	+	+	+	+	-	-
2	+	+	-	+	+	+
3	+	+	-	-	-	-
4	+	+	+	-	+	+
5	-	-	+	+	-	-
6	-	-	-	+	+	+
7	-	-	-	-	-	-
8	-	-	+	-	+	+
9	+	-	+	+	-	+
10	+	-	-	+	+	-
11	+	-	-	-	-	+
12	+	-	+	-	+	-
13	-	+	+	+	-	+
14	-	+	-	+	+	-
15	-	+	-	-	-	+
16	-	+	+	-	+	-
17	-	-	+	+	+	+
18	-	-	-	+	-	-
19	-	-	-	-	+	+
20	-	-	+	-	-	-
21	+	+	+	+	+	+
22	+	+	-	+	-	-
23	+	+	-	-	+	+
24	+	+	+	-	-	-
25	-	+	+	+	+	-
26	-	+	-	+	-	+
27	-	+	-	-	+	-
28	-	+	+	-	-	+
29	+	-	+	+	+	-
30	+	-	-	+	-	+
31	+	-	-	-	+	-
32	+	-	+	-	-	+

When $i = 16$, the CAL and SAL waveforms become hard limited cosine and sine waveforms, respectively, but it is not possible to represent both waveforms simultaneously with 32 time-coincident, nonzero sample values. A filter can be built for the $i = 16$ case by the introduction of suitable sampling delays, but this was inconvenient for our simulation model, so no data were obtained for this case. The above argument also applies for other values of N to the filter for which $i = N/2$; it being presumed that only even values of N are considered.

For the N-point transform processor being discussed here, a negative input frequency of $-f(|f| < 0.5f_s)$ cannot be distinguished from a positive input frequency of $N - f$. Therefore, it suffices to calculate the filter responses by letting the frequency variable f run from zero to N, keeping in mind that the input frequency would equal f for $f < \frac{N}{2}$, whereas the input frequency would actually be $f - N$ for values of f greater than $N/2$.

In order to compute the responses of the ith filter, let

$$t_k = \frac{k}{N}, \; k = 0, 1, ---N-1 \quad . \tag{6}$$

Expressing the input signal in complex form as

$$S(t_k) = \mathrm{EXP}[j(2\pi f t_k + \phi)] \, , \tag{7}$$

the complex output voltage $V(i, f, N)$ will be given by

$$V(i,f,N) = \frac{1}{N} \sum_{k=0}^{N-1} S(t_k) A(t_k) [W_c(i,t_k) - jW_s(i,t_k)]$$

$$= \frac{1}{N} e^{i\phi} \sum_{k=0}^{N-1} [(H_1(i,f,N) + H_3(i,f,N) + j(H_2(i,f,N) - H_4(i,f,N))] \, , \tag{8}$$

where

$$H_1 = H_1(i,f,N) = \frac{1}{N} \sum_{k=0}^{N-1} A(t_k)\, W_c(i,t_k) \cos(2\pi f t_k) \qquad (9)$$

$$H_2 = H_2(i,f,N) = \frac{1}{N} \sum_{k=0}^{N-1} A(t_k)\, W_c(i,t_k) \sin(2\pi f t_k) \qquad (10)$$

$$H_3 = H_3(i,f,N) = \frac{1}{N} \sum_{k=0}^{N-1} A(t_k)\, W_s(i,t_k) \sin(2\pi f t_k) \qquad (11)$$

$$H_4 = H_4(i,f,N) = \frac{1}{N} \sum_{k=0}^{N-1} A(t_k)\, W_s(i,t_k) \cos(2\pi f t_k) \; . \qquad (12)$$

The output signal power P is computed from

$$P(i,f,N) = |V(i,f,N)|^2 \qquad (13)$$

and $Z = 10 \log_{10} P$ will be plotted as a function of i, f, and N. No attempt will be made to normalize the peak response in any filter to a value Z = 0 since the benefit gained is not worth the programming effort required – actually the peak responses are all clustered very close to 0 dB.

Because of the assumed unit duration of the observation interval, the incremental value chosen for f was 0.2. The computations were carried out using double precision arithmetic, and the values of Z were rounded to one decimal place before being printed out. For the circular correlation waveforms, the quantization levels used were 0, 1, 2, 4, 8, and (theoretically) infinite amplitude bits.

4.0 DISCUSSION OF RESULTS

4.1 32-POINT TRANSFORM

4.1.1 Fourier Processing, No Quantizing

Figures 2, 3, and 4 illustrate filter transfer functions for Fourier processing with no quantizing of the reference waveforms. These curves are very typical of the response curves obtained for other filter center frequencies, and no further elaboration is necessary in this section beyond noting that, with Hamming weighting, all filter sidelobes were at least 40 dB below the filter mainlobe.

4.1.2 Walsh Processing

Figures 5 through 14 show typical response curves for Walsh processing with Hamming data weighting; their most striking feature is the introduction of numerous high-level spurious sidelobes or artifacts, as they will be called throughout the rest of this report. These artifacts arise from the sharp transitions between the positive and negative values of the Walsh reference waveforms. A comparison of Figs. 11 and 15 shows the minimal effect of the choice of data weighting upon the artifact structure. This is to be expected, since the data weighting is effective as a "transition smoother" only at the beginning and end of the processing time interval, whereas the Walsh reference waveforms introduce step function transitions throughout the processing time interval.

Although not presented here, response data were collected for other filter center frequencies so that, for the case of Hamming weighting, a complete data base exists for center frequencies from 1 through 15. Examination of these data leads to the following observations concerning Walsh processing with Hamming data weighting:

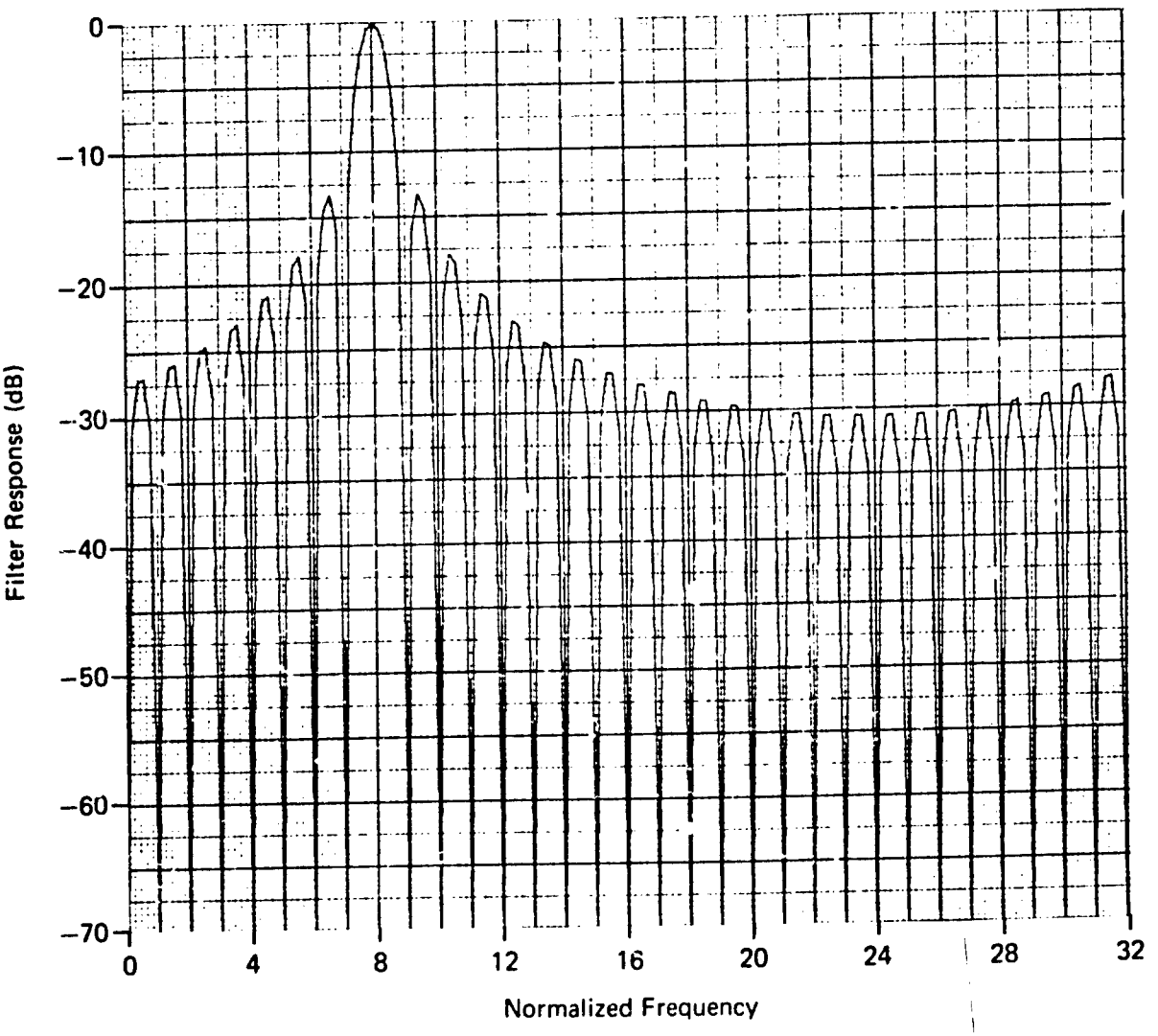

Fig. 2 Uniform Weighting Fourier Processing; N = 32, f_0 = 8

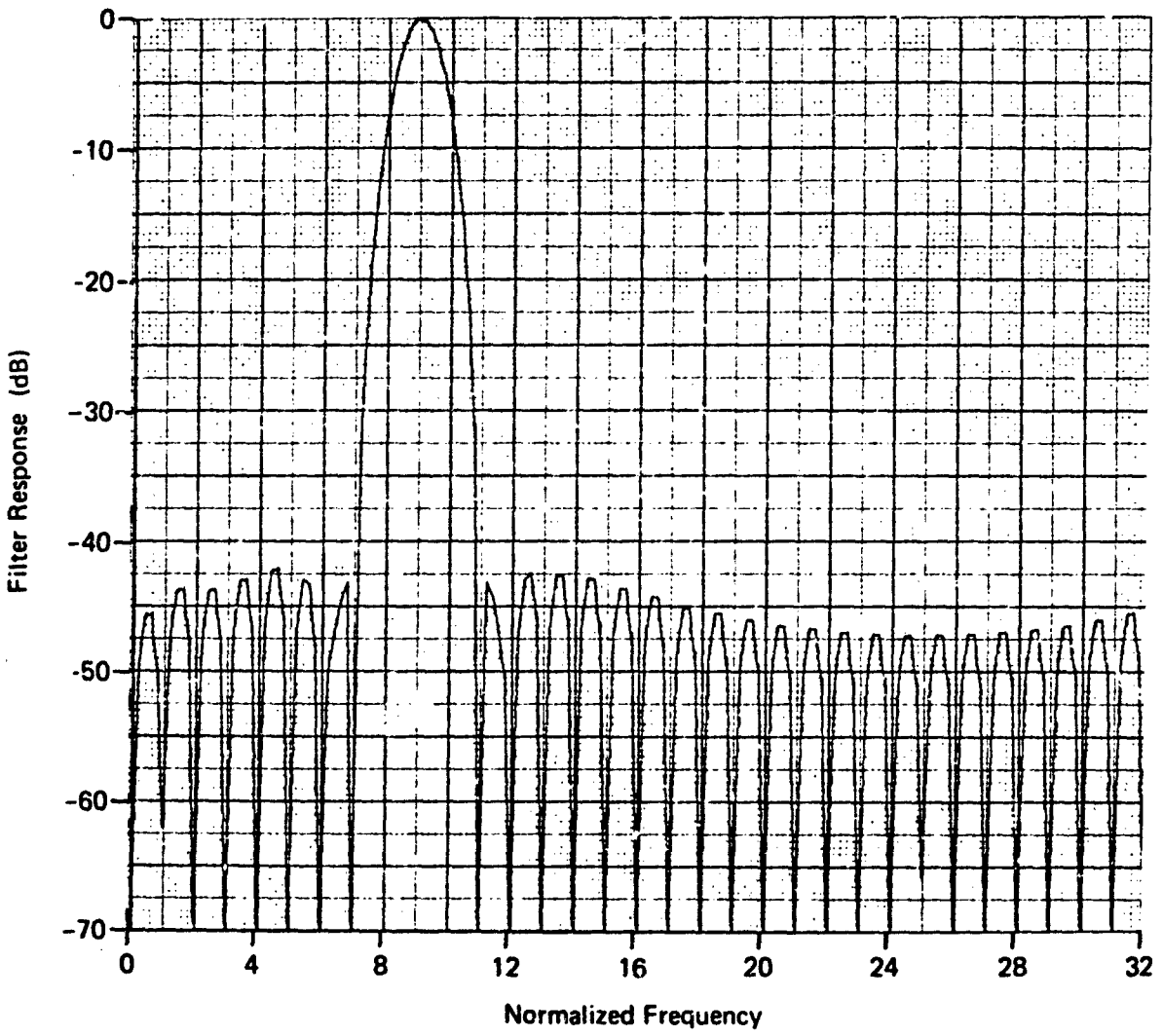

Fig. 3 Hamming Weighting Fourier Processing; N = 32, f_0 = 8

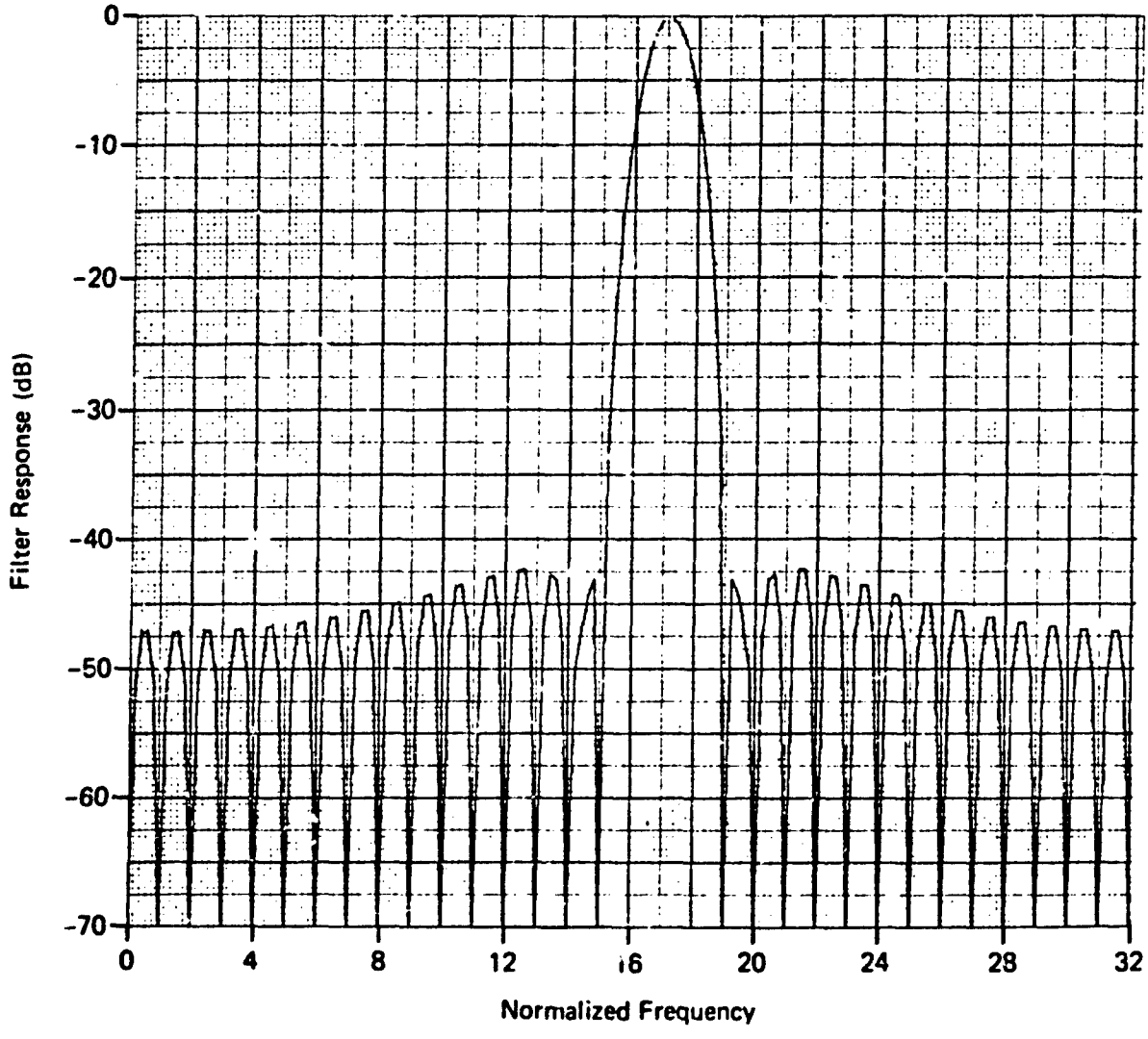

Fig. 4 Hamming Weighting Fourier Processing; N = 32, f_0 = -15

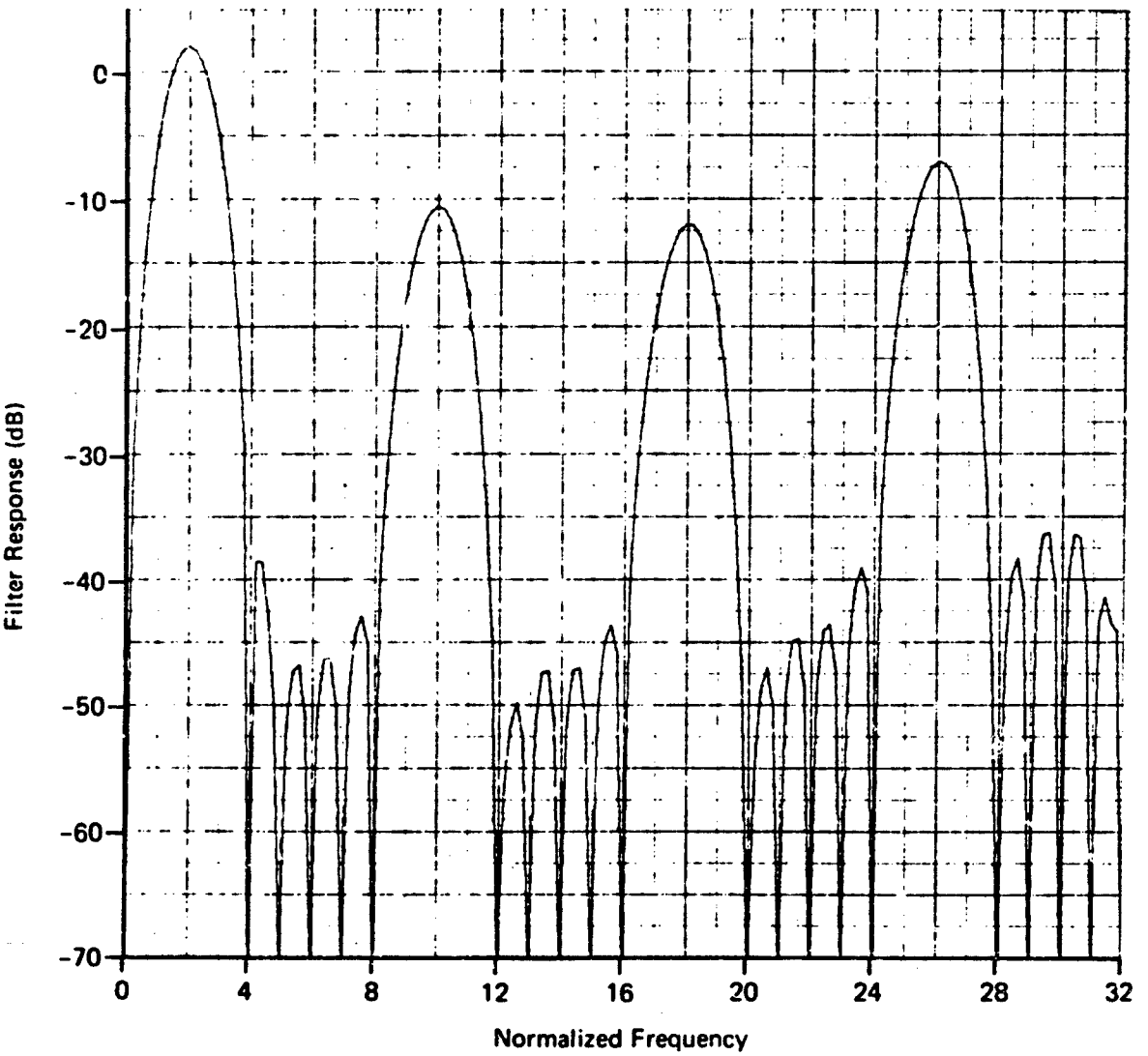

Fig. 5 Hamming Weighting Walsh Processing; N = 32, $f_0 = 2$

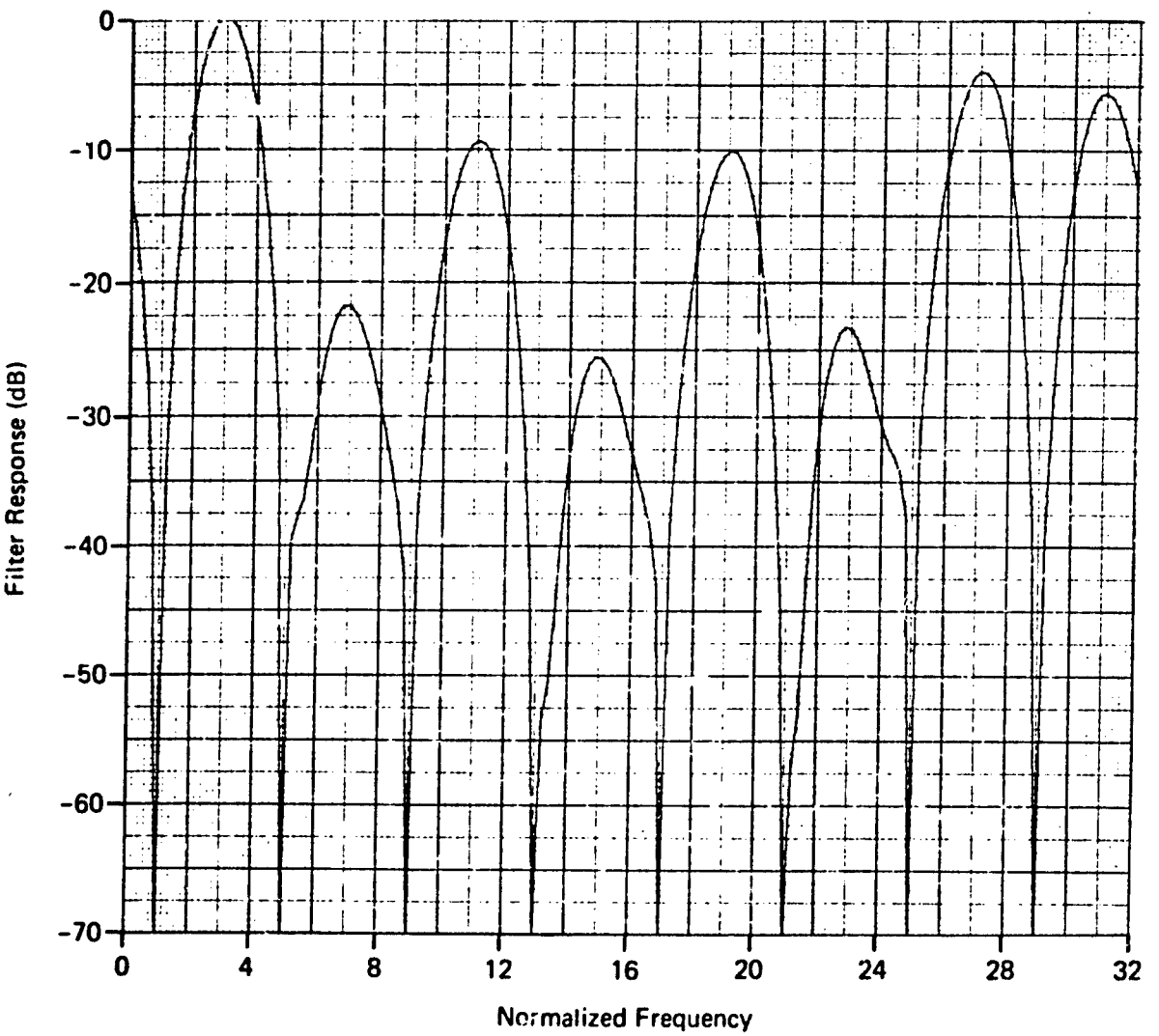

Fig. 6 Hamming Weighting Walsh Processing; N = 32, f_0 = 3

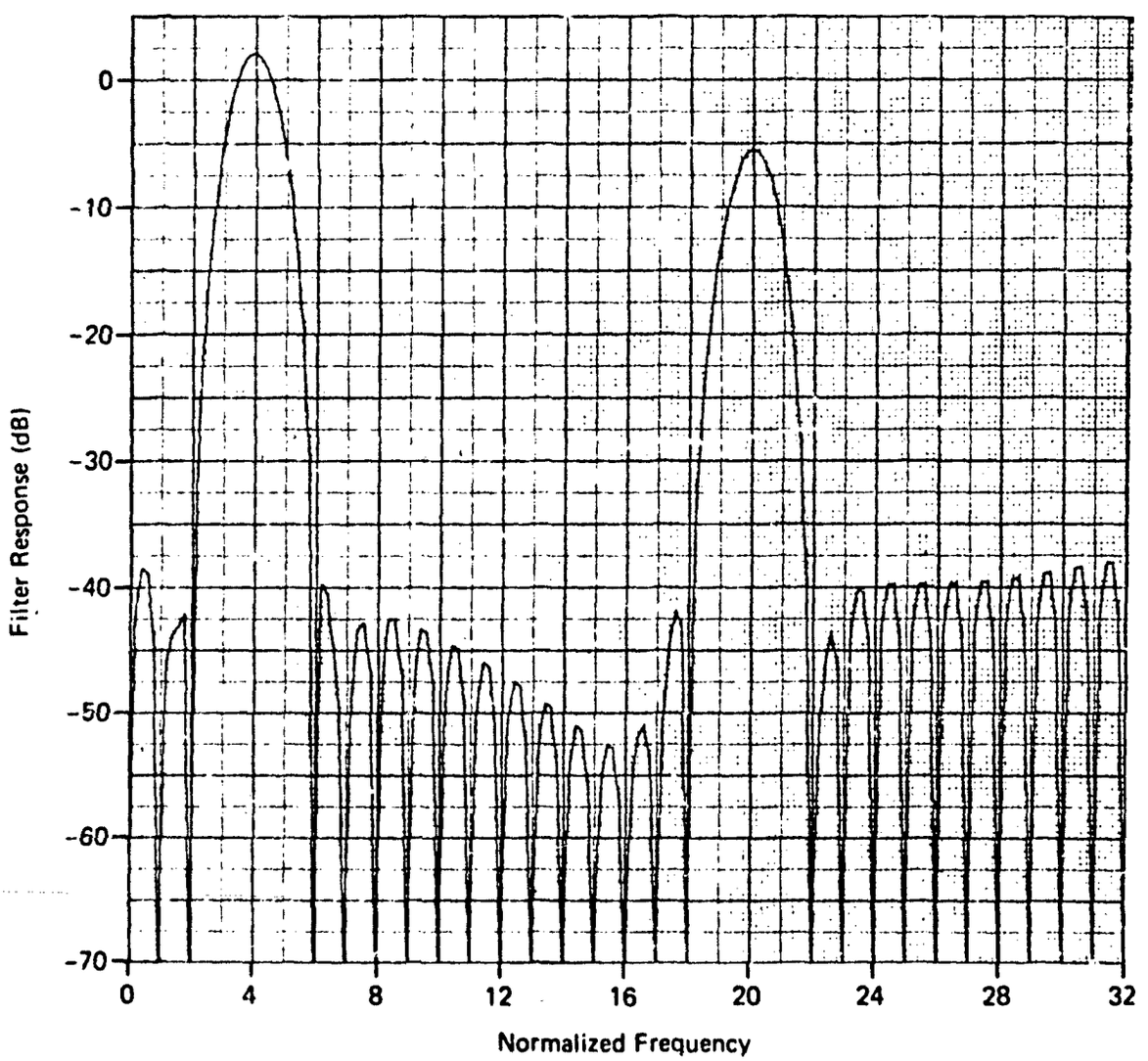

Fig. 7 Hamming Weighting Walsh Processing; N = 32, f_0 = 4

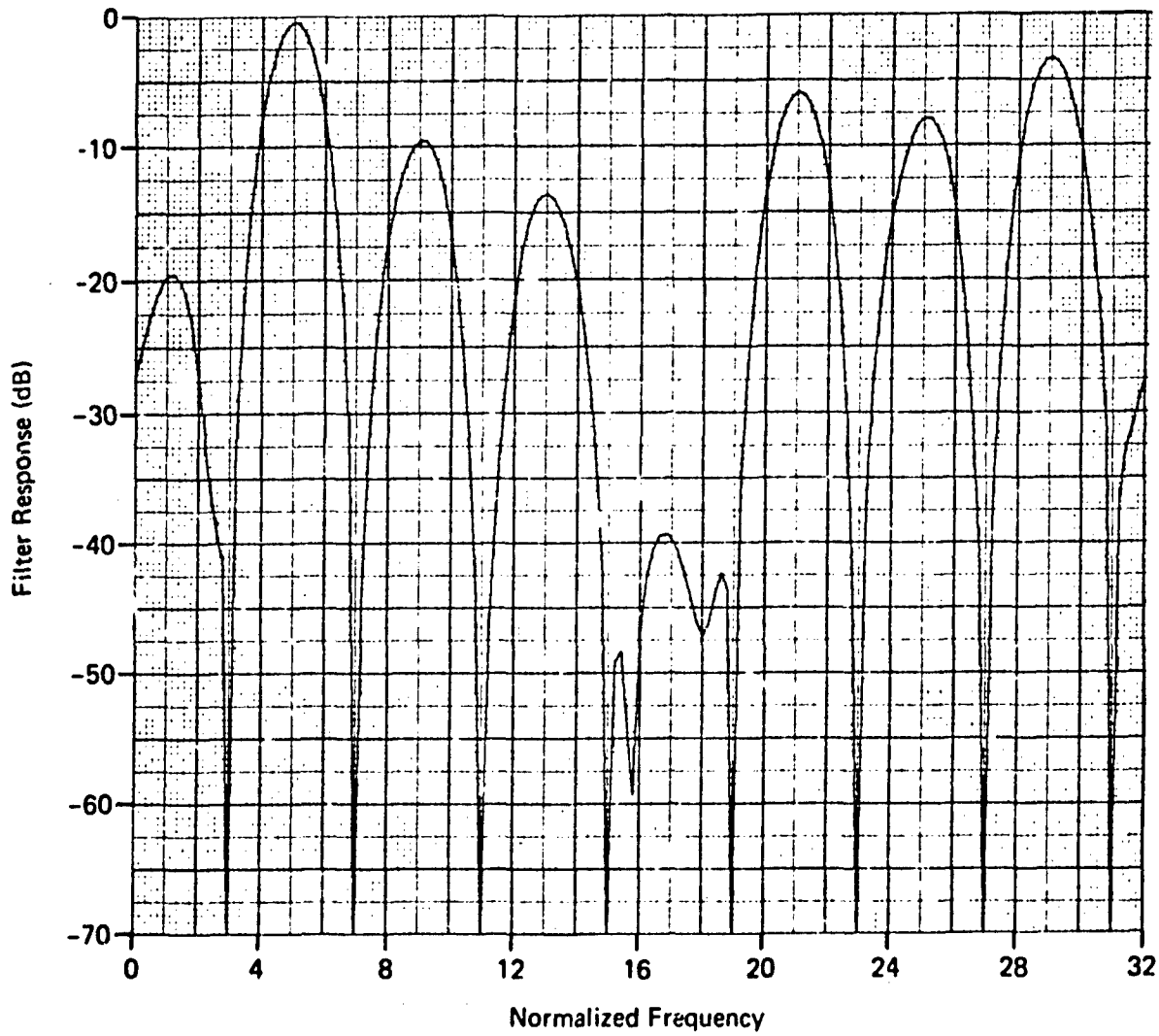

Fig. 8 Hamming Weighting Walsh Processing; N = 32, f_0 = 5

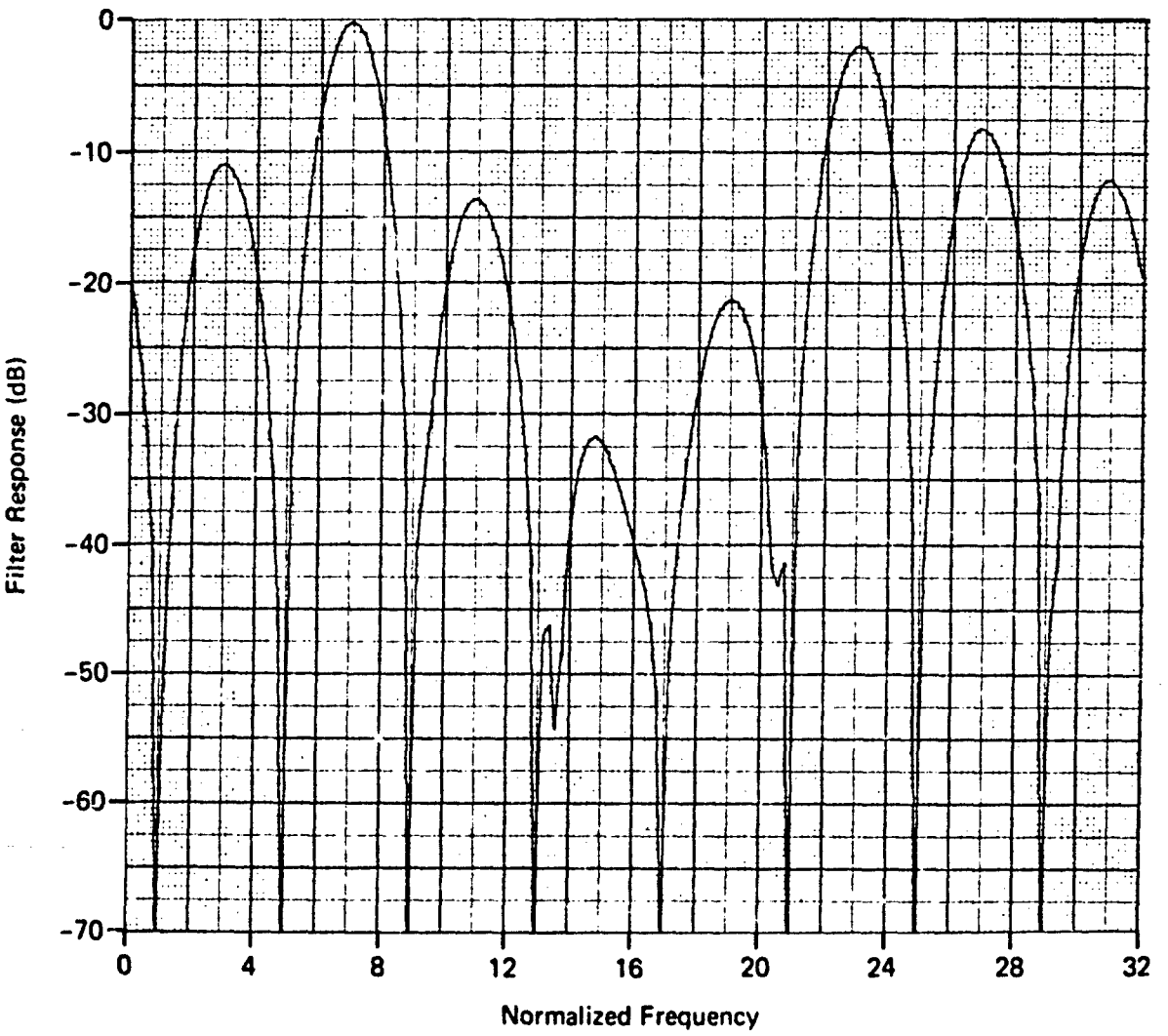

Fig. 9 Hamming Weighting Walsh Processing; N = 32, f_0 = 7

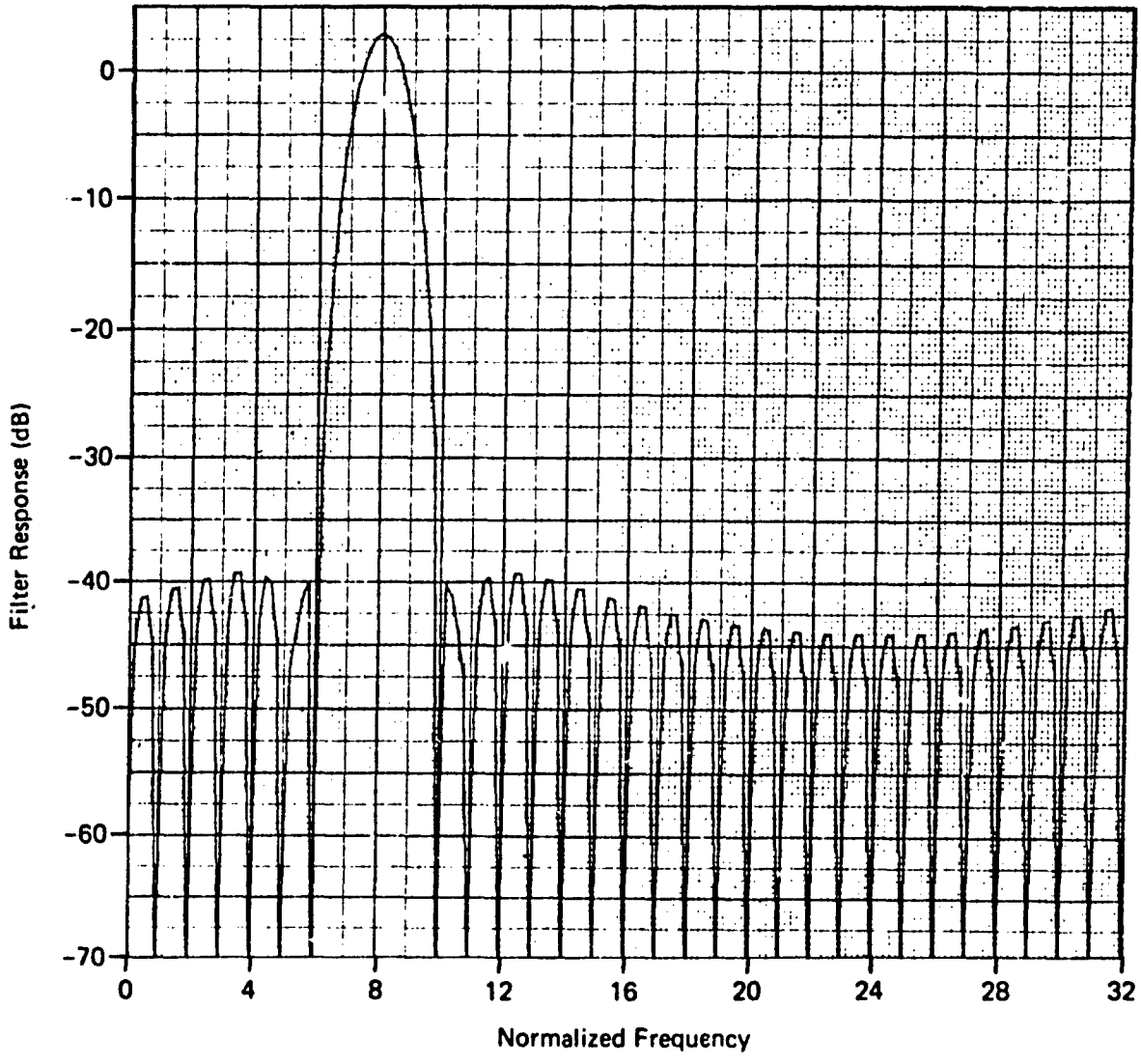

Fig. 10 Hamming Weighting Walsh Processing; N = 32, $f_0 = 8$

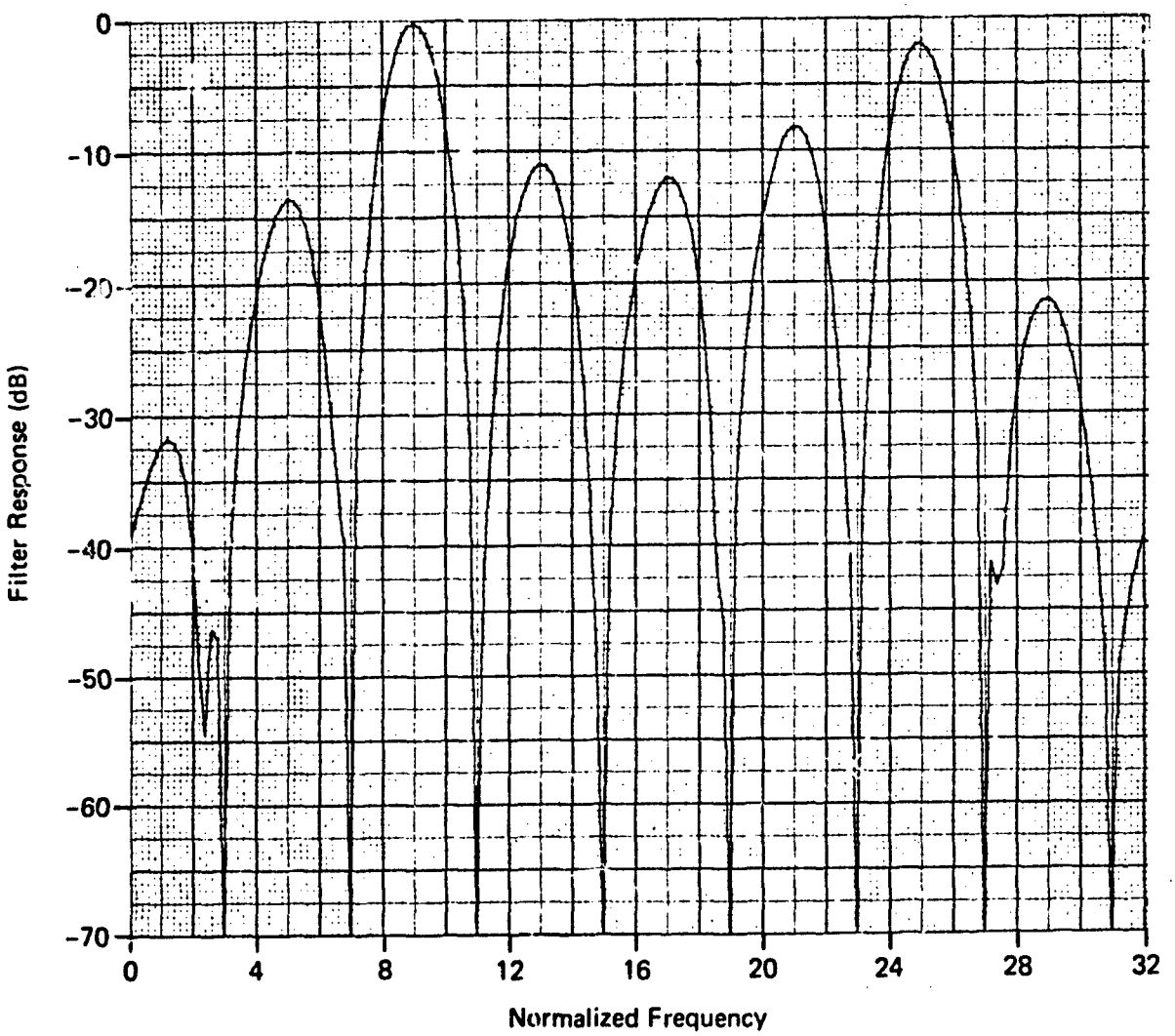

Fig. 11 Hamming Weighting Walsh Processing; N = 32, f_0 = 9

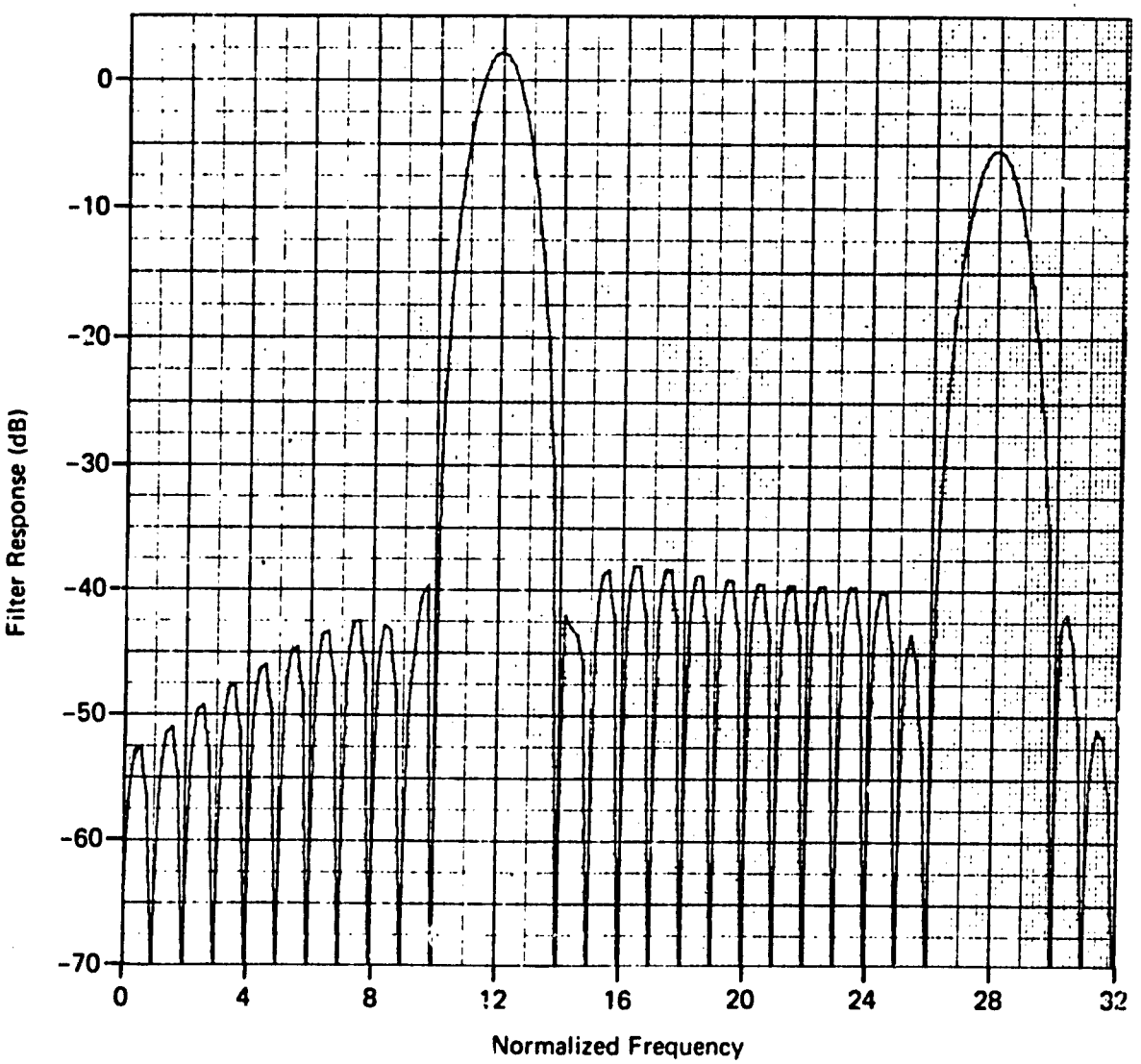

Fig. 12 Hamming Weighting Walsh Processing; N = 32, f_0 = 12

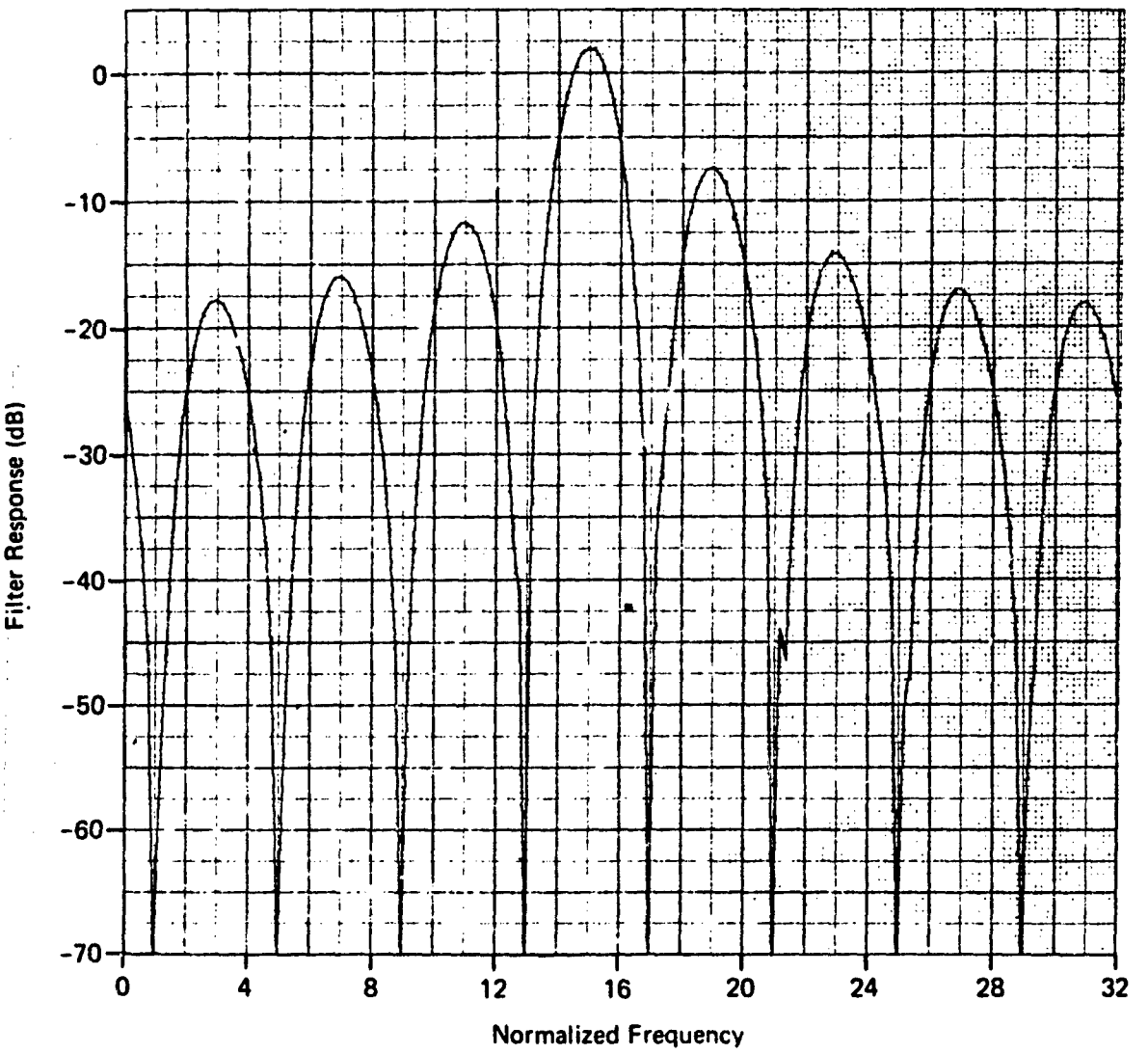

Fig. 13 Hamming Weighting Walsh Processing, N = 32, f_0 = 15

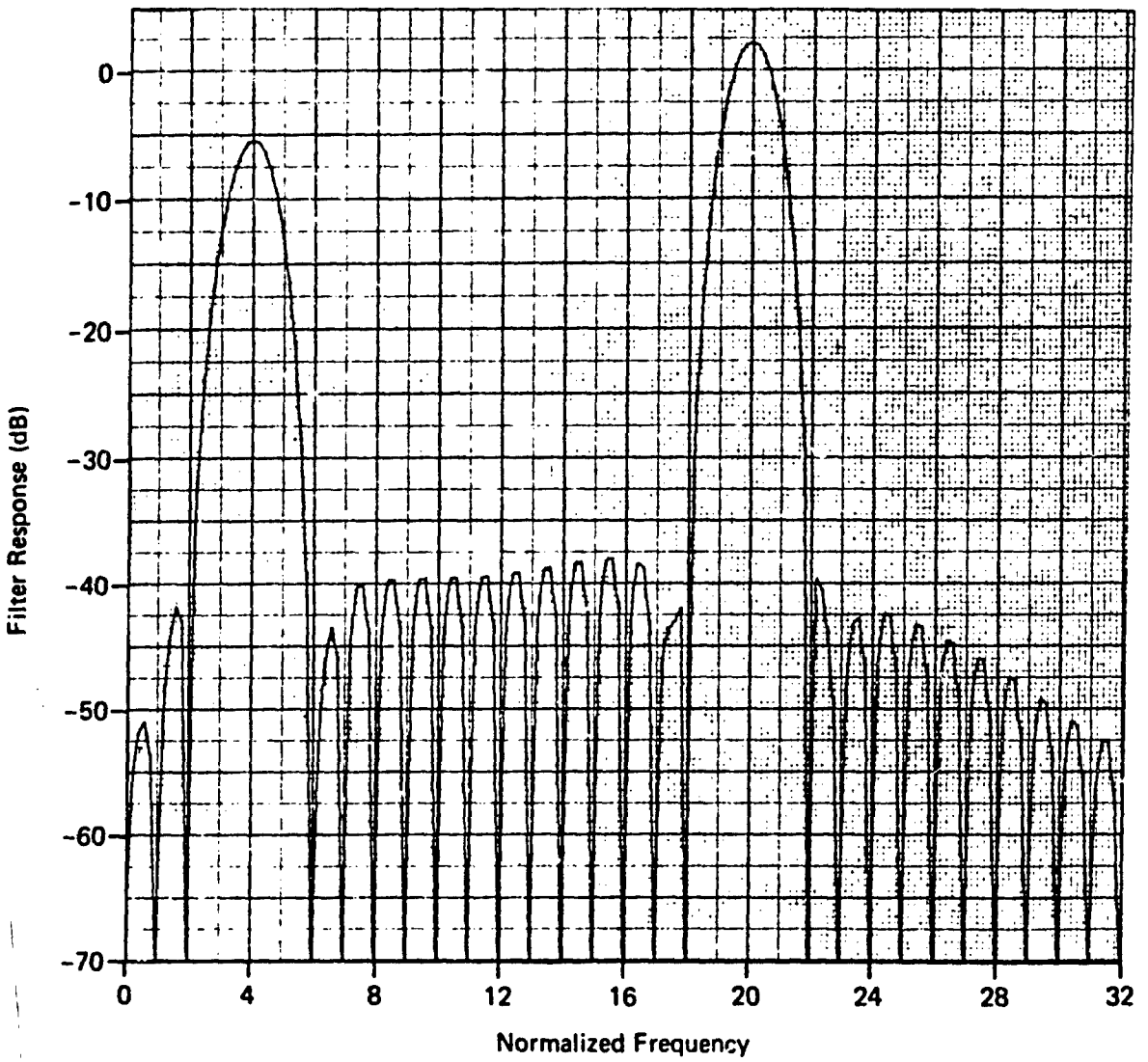

Fig. 14 Hamming Weighting Walsh Processing; N = 32, f_0 = -12

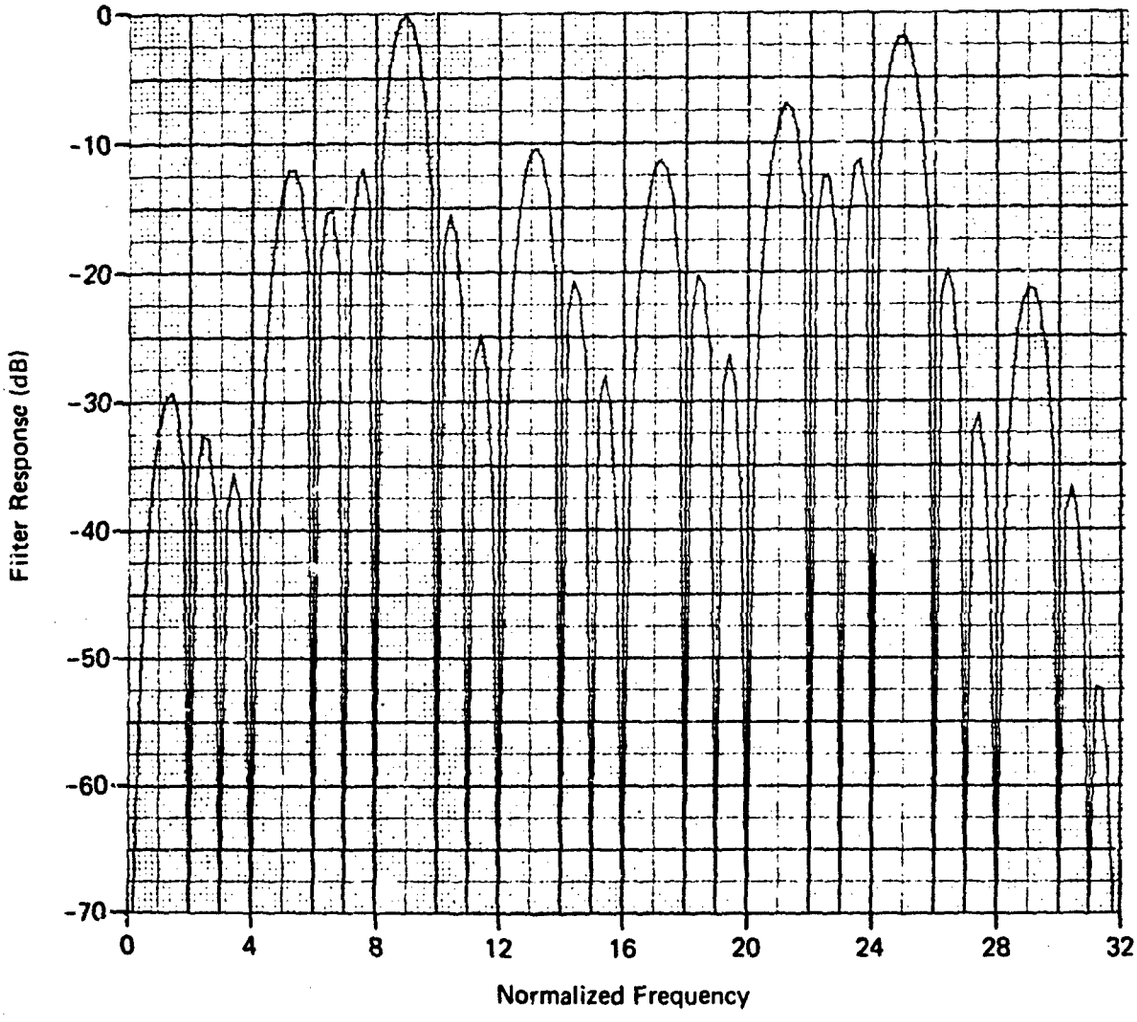

Fig. 15 Uniform Weighting Walsh Proecessing; N = 32, f_0 = 9

1. The peak artifact level encountered was 1.7 dB below a filter mainlobe response. For the data subset denoted by $i = 1, 2, 4$ the peak level was 7.6 dB down.

2. In the case of Hamming data weighting, the number of artifacts exceeding -30 dB was 66. For the cases $i = 1, 2$, and 4 the median level was -13.9 dB; the average number of artifacts per filter was 3.7. For the other values of i the median level was -10.7 dB; the average number of artifacts per filter was 5.0.

3. As a general rule, the filters having even numbered center frequencies have fewer artifacts than those having odd numbered center frequencies.

4. For the filter having a center frequency of 8, there were no artifacts. This is to be expected, since the sampled values of the reference waveforms in the case are the same as for unquantized Fourier processing. See also Figs. 3 and 10.

5. Contrary to earlier expectations, the number of the artifacts do not tend to decrease with increasing filter center frequencies except for the cases $i = 1, 2$, and 4.

6. With Hamming weighting, the artifact width is approximately equal to that of the mainlobe, and the maximum number of artifacts observed in a given filter was 7.0. With uniform weighting the artifact structure is somewhat complicated by interference from the ordinary filter minor lobes.

7. There was no observed tendency for artifact lobes to avoid the regions around $f = 0$ and

f = 32. The implications of this in the radar clutter rejection problem are obvious.

8. Every filter had a single mainlobe at the correct center frequency whose width was commensurate with the form of data weighting used.

9. The interartifact sidelobe level was comparable to that obtained using Fourier processing, except in those cases where the number of artifacts was so large as to leave no room for interartifact minor lobes.

4.1.3 Quantized Fourier Processing

Hard Limited Case. For purposes of comparison with the results obtained using Walsh processing, we have prepared an analogous data base and a set of response curves (Figs. 16-24) for the Fourier processing situation in which the circular reference waveforms are hard limited. Denoting the original waveform by the general symbol F(t) and the hard-limited waveform by the symbol $F_L(t)$, we will have

$$F_L(t) = \begin{cases} +1, F(t)>0 \\ 0, F(t)=0 \\ -1, F(t)<0 \end{cases} \qquad (13)$$

and we note that now the value zero is permitted for a reference waveform value, whereas for Walsh processing only the values +1 and -1 were allowed.

Examination of the filter response results shows that the artifact problem remains, as was to be expected, but is reduced in seriousness from the point of view of size and number. The comparative situation is summarized in Table 2, which covers those artifact levels exceeding the -30 dB level, with Hamming data weighting

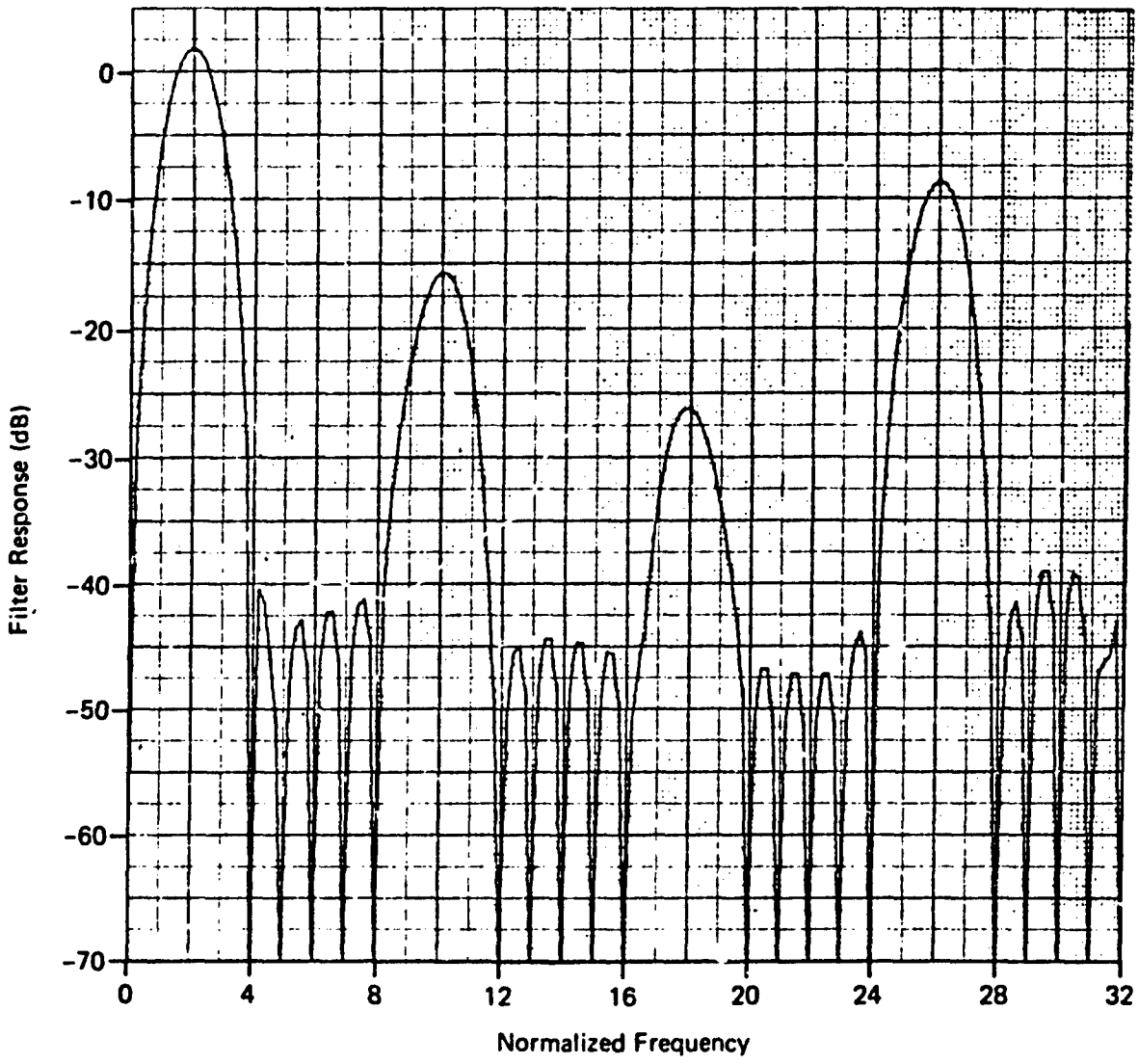

Fig. 16 Hamming Weighting 0-bit Fourier Processing; N = 32, $f_0 = 2$

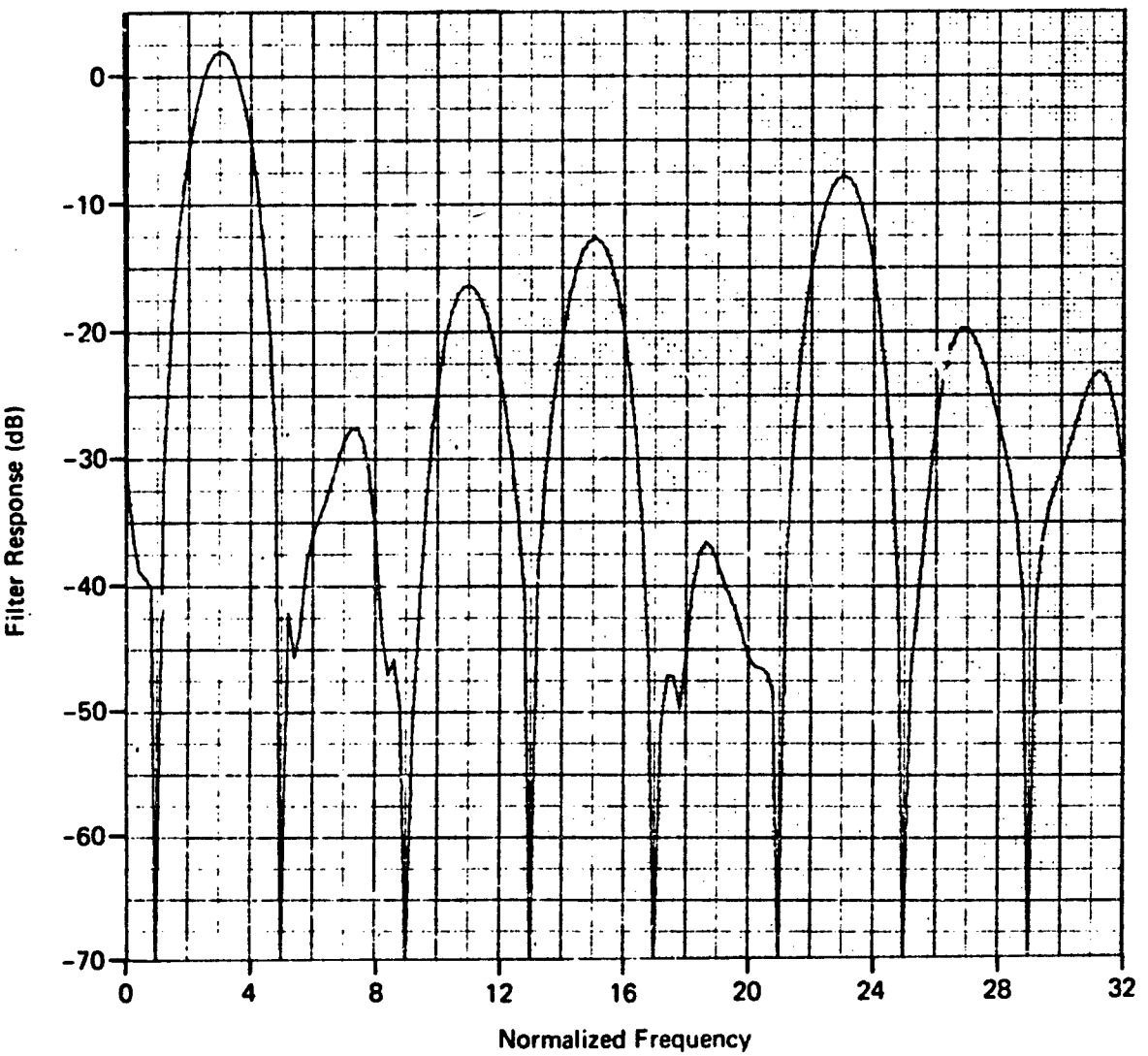

Fig. 17 Hamming Weighting 0-bit Fourier Processing; N = 32, $f_0 = 3$

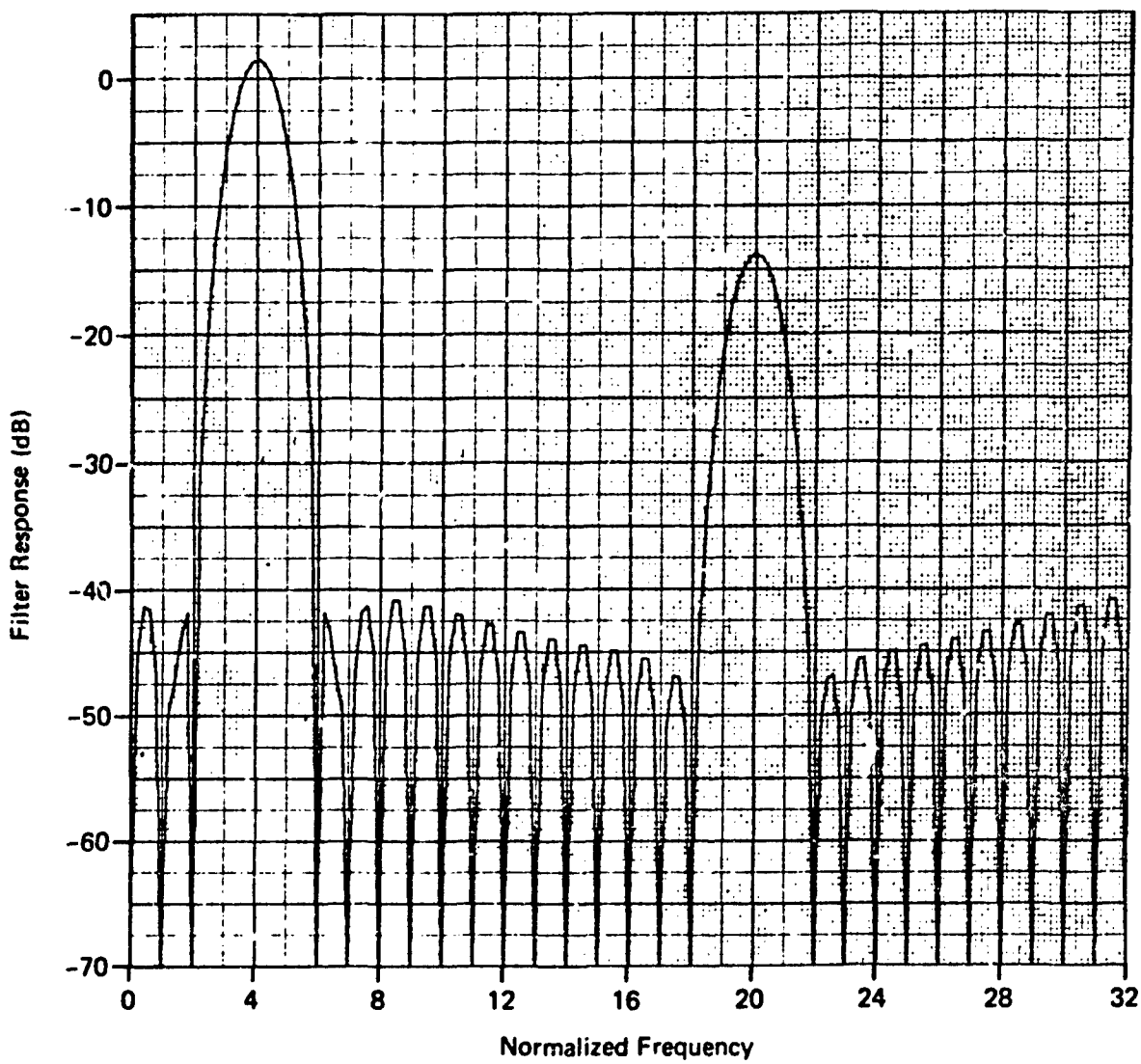

Fig. 18 Hamming Weighting 0-bit Fourier Processing; N = 32, f_0 = 4

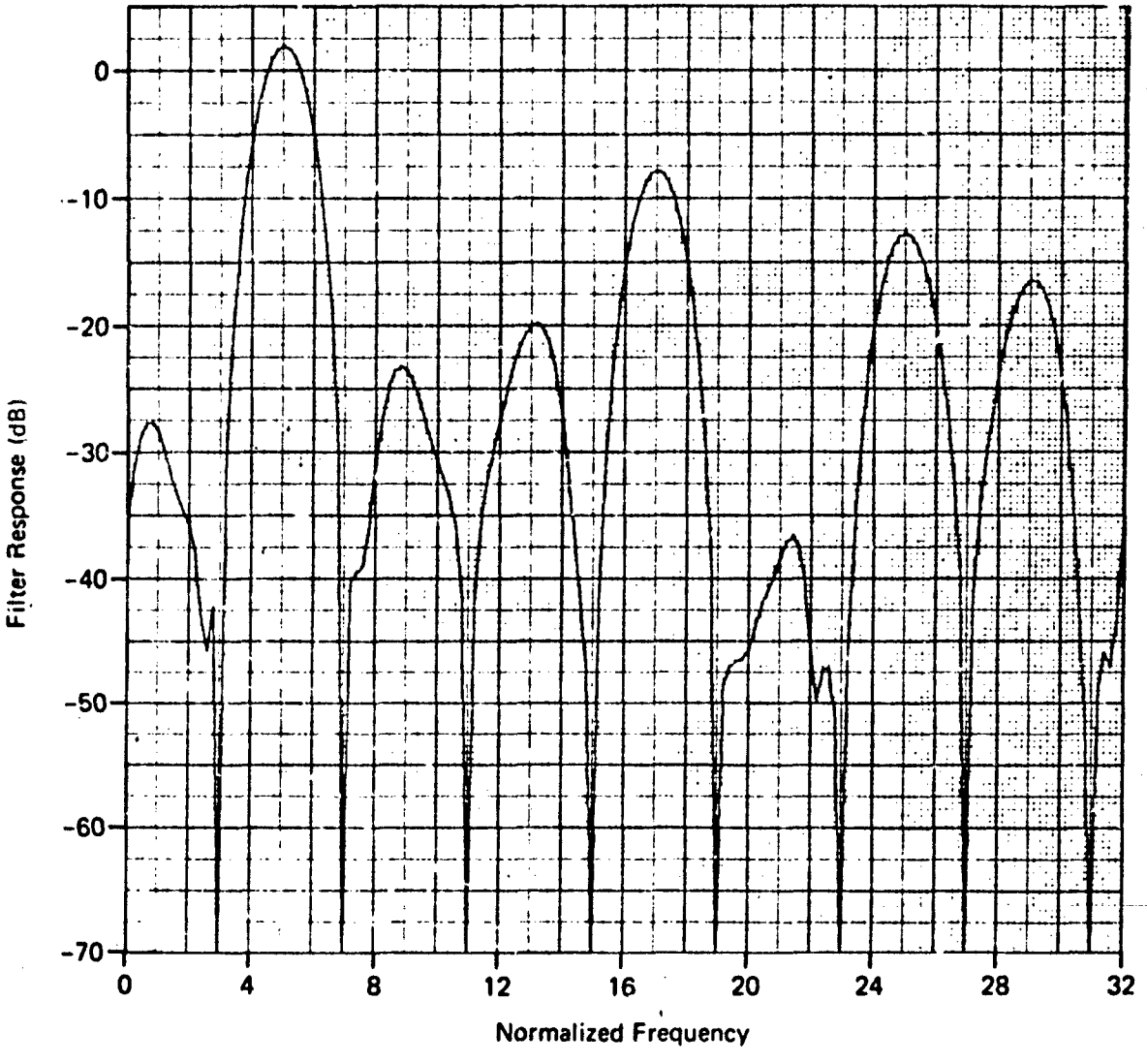

Fig. 19 Hamming Weighting 0-bit Fourier Processing; N = 32, f_0 = 5

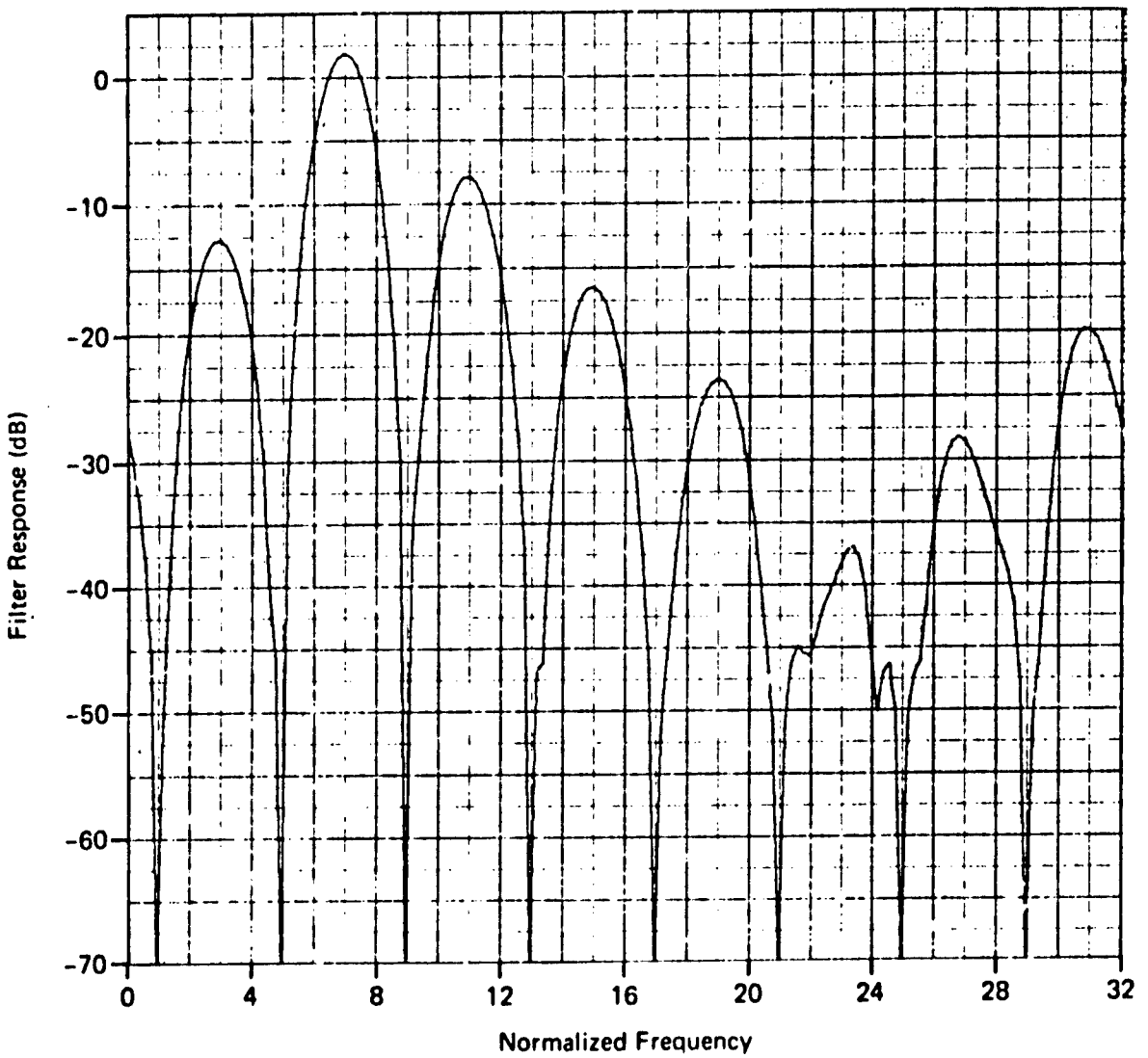

Fig. 20 Hamming Weighting 0-bit Fourier Processing; N = 32, f_0 = 7

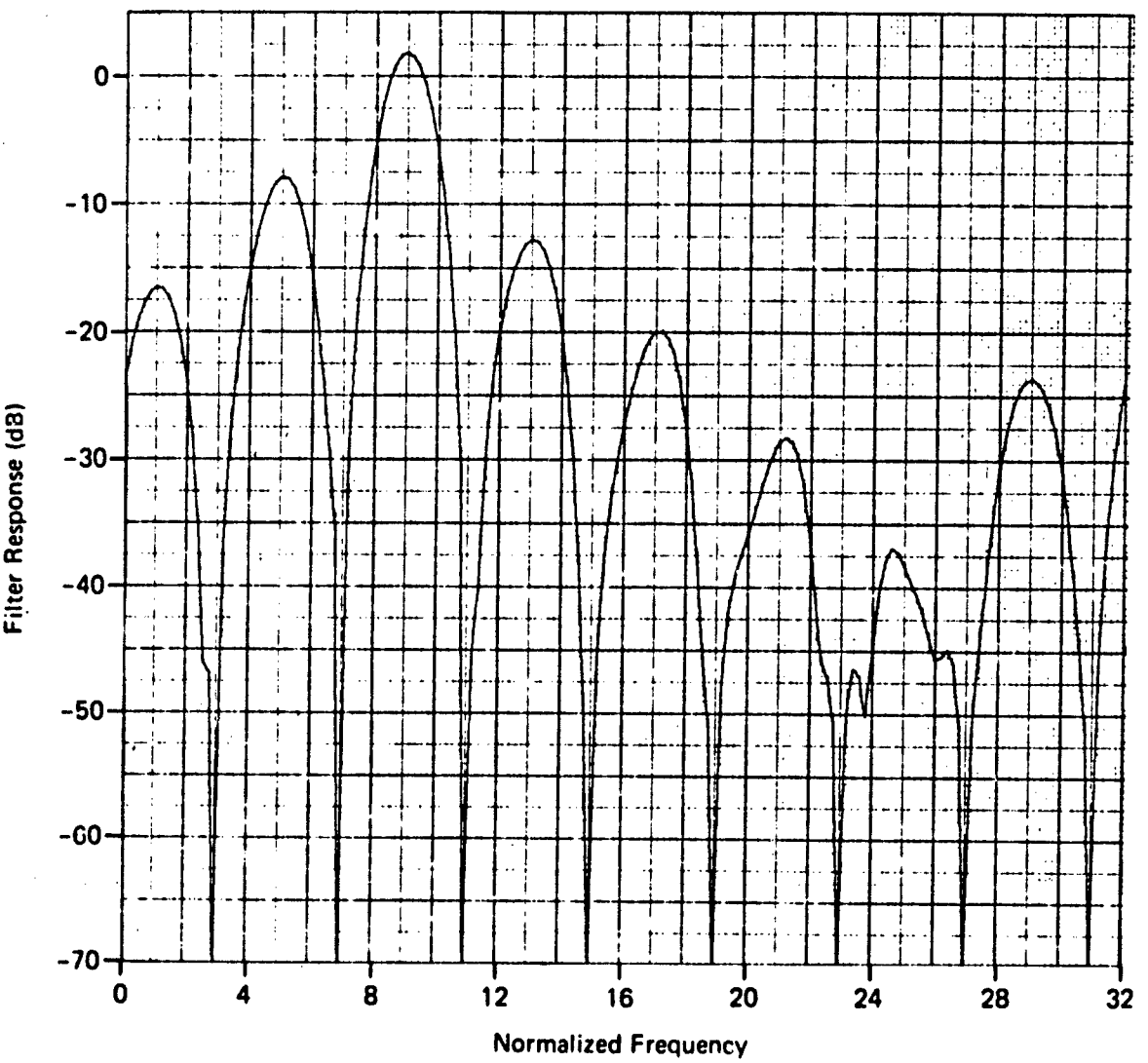

Fig. 21 Hamming Weighting 0-bit Fourier Processing; N = 32, f_0 = 9

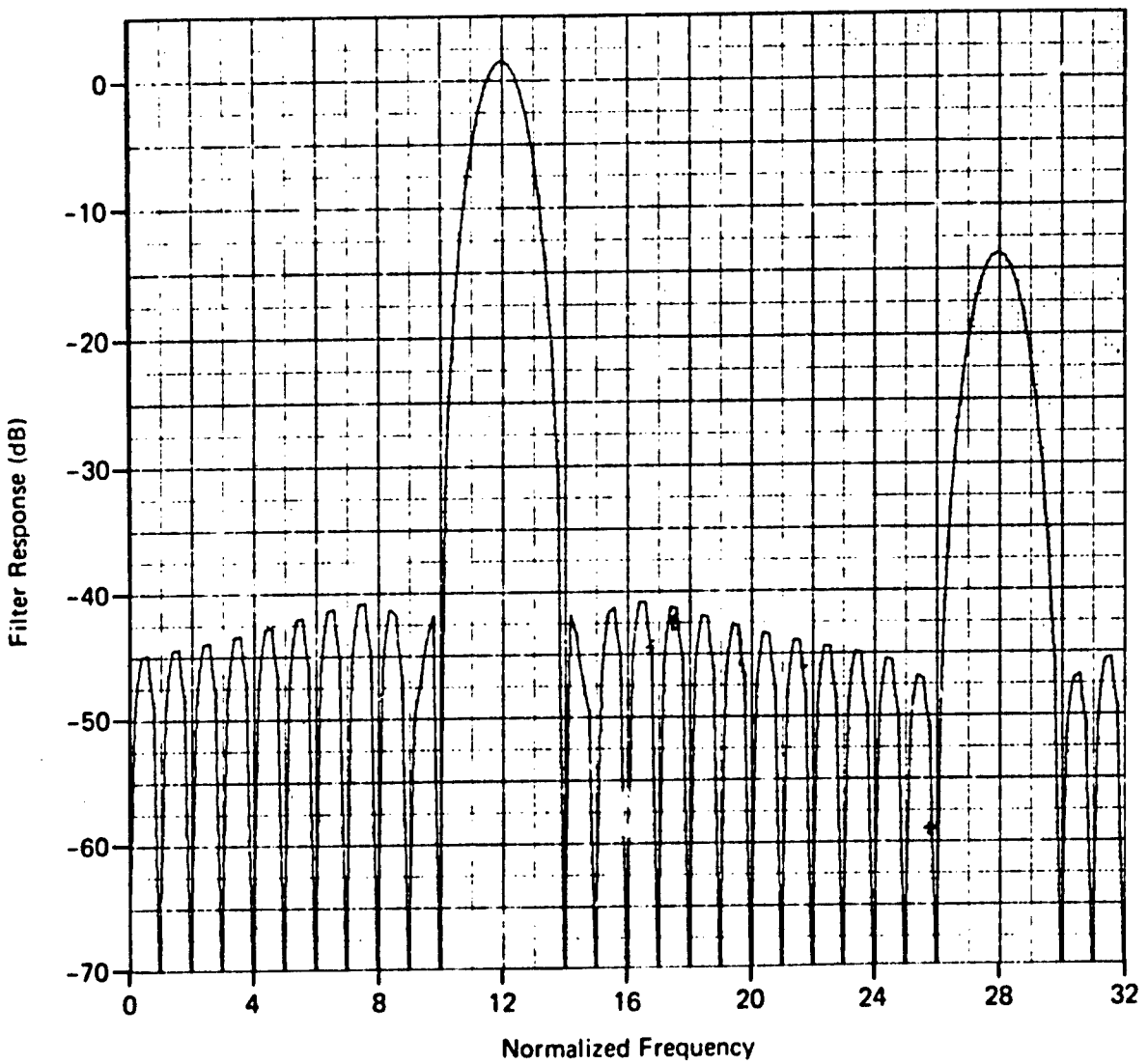

Fig. 22 Hamming Weighting 0-bit Fourier Processing; $N = 32$, $f_0 = 12$

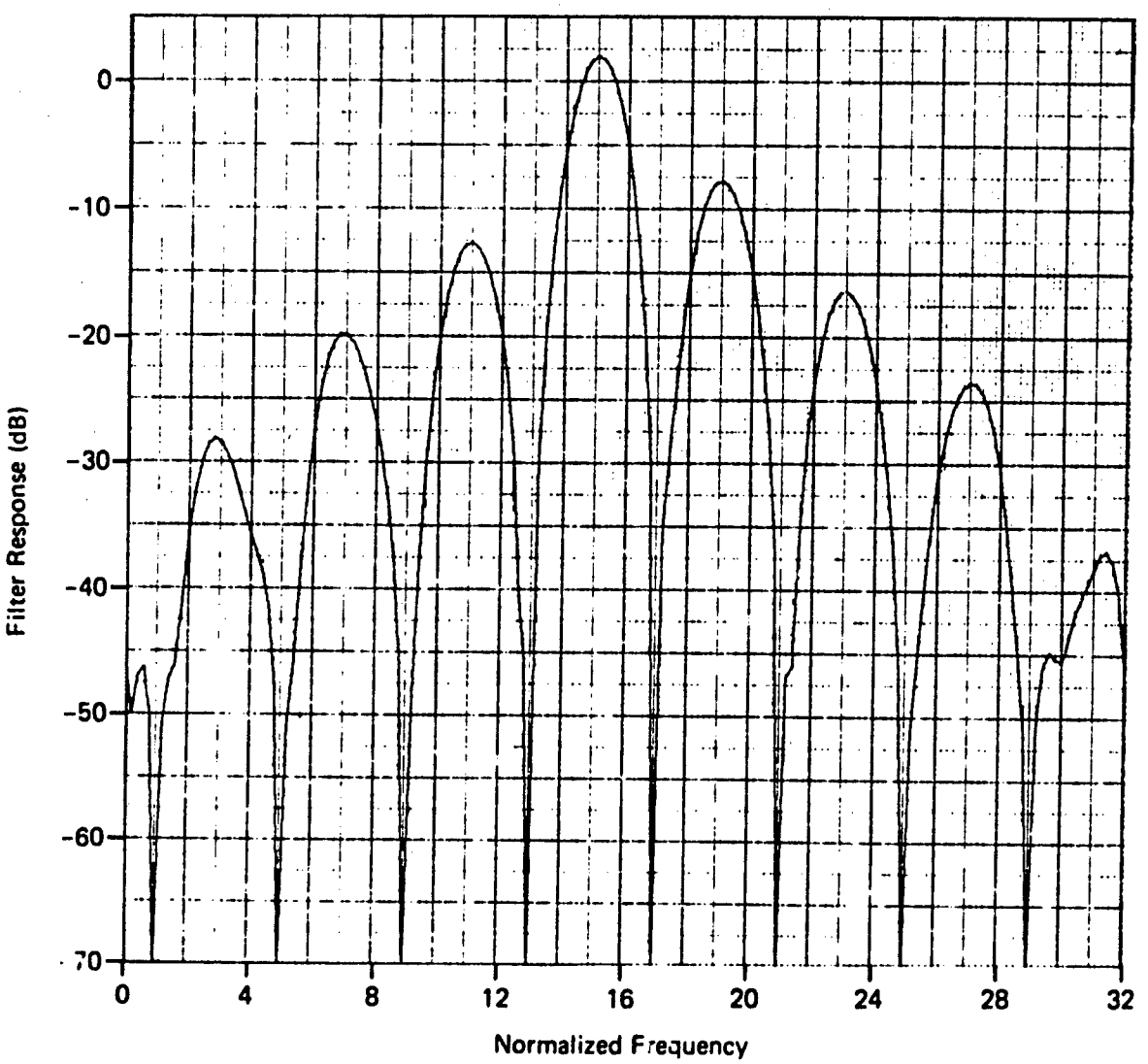

Fig. 23 Hamming Weighting 0-bit Fourier Processing; N = 32, f_0 = 15

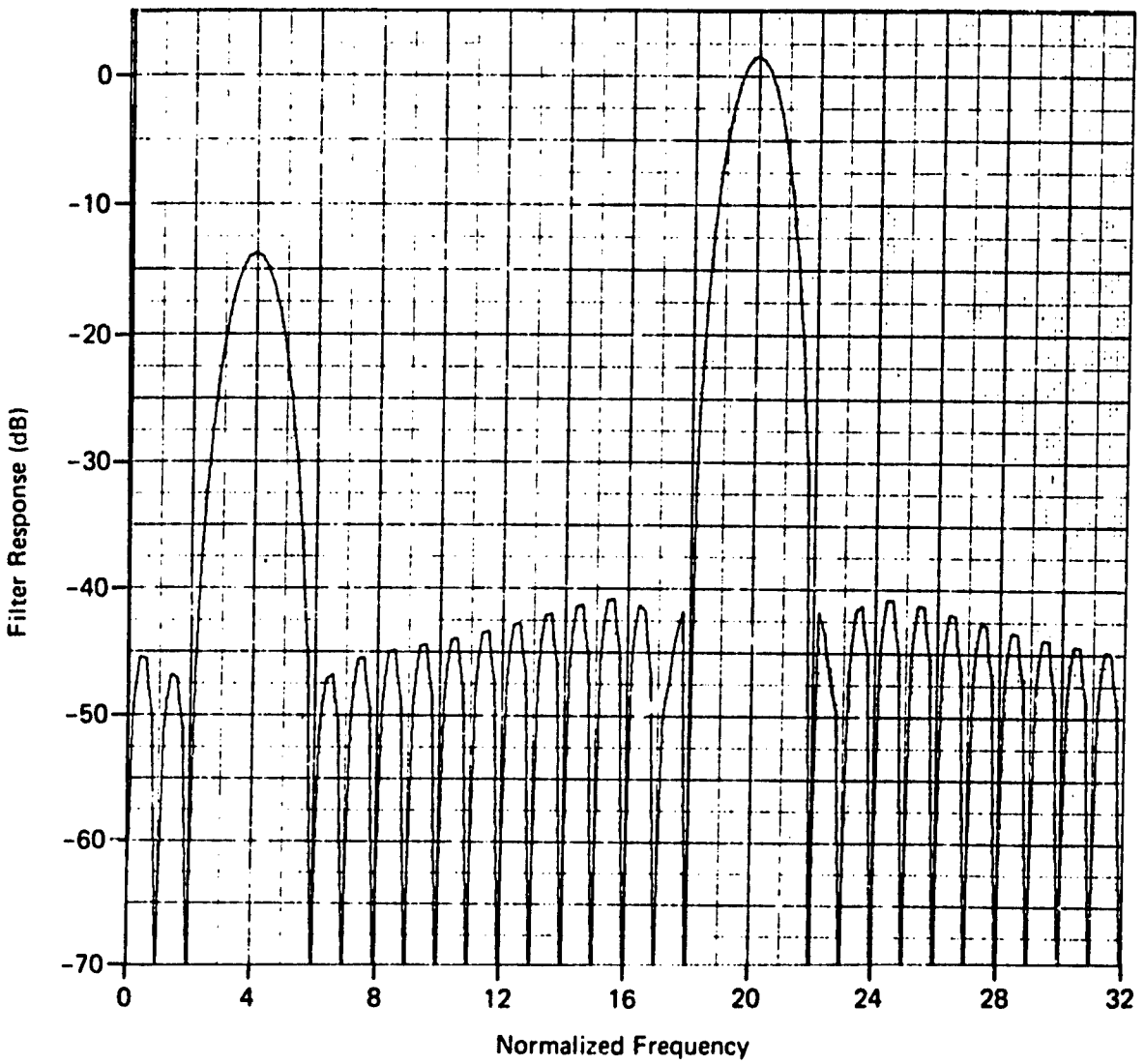

Fig. 24 Hamming Weighting 0-bit Fourier Processing; N = 32, f_0 = -12

Table 2

Artifact Level Distribution, 32-Point Transforms, Filters 1-15

Peak Artifact Level below Mainlobe (dB)	Walsh		Hard Limited Fourier	
	Number	Fraction	Number	Fraction
0-3	4	0.06	0	0
3-6	8	0.12	0	0
6-9	8	0.12	0	0
9-12	14	0.21	12	0.21
12-15	10	0.15	8	0.14
15-18	4	0.06	6	0.11
18-21	10	0.15	8	0.14
21-24	6	0.09	8	0.14
24-27	2	0.03	8	0.14
27-30	0	0	7	0.12
Total	66	1.0	57	1.0

being assumed. Note particularly that the Walsh transform produced 16% more artifacts, and that they are concentrated at higher levels.

With the exception of Observation No. 1, (where 1.7 dB should be replaced by 9.8 dB), and Observation No. 2 (Section 4.1.2), all the observations apply without modification in the case of hard-limited Fourier processing. To these seven comments, one more should be added, and that is that, since Observation No. 8 is applicable, it is obviously unnecessary, for the filtering configuration analyzed here, that the members of a correlation waveform set form a complete set in the mathematical sense, since the hard-limited circular set used here does not form a complete set.

Nonhard Limited Cases. Filter response data were also obtained for center frequencies from 1 through 15 for the cases where the amplitude levels of the reference waveforms were quantized to 1, 2, 4, and 8 bits and Hamming data weighting was used. As the number of bits is increased, the artifact levels are reduced. The 8-bit response curves cannot be easily distinguished from those using infinite bits; that is, no quantizing at all. Figures 21 and 25 through 28 illustrate the progressive decay of the artifacts with increasing numbers of bits.

In Ref. 5 the authors investigated and tabulated the peak artifact levels that would be expected in a 64-point DFT as a function of the number of amplitude bits used to represent reference waveforms. Our 32-point transform results are, for the cases of 0, 1, 2, and 4-bit quantizing, in excellent agreement with those in Ref. 5, as an examination of Table 3 will show. For the 8-bit case, a comparison cannot be made because the peak level from Ref. 5 is -60.4 dB, which is well below the sidelobe level obtained without any quantizing.

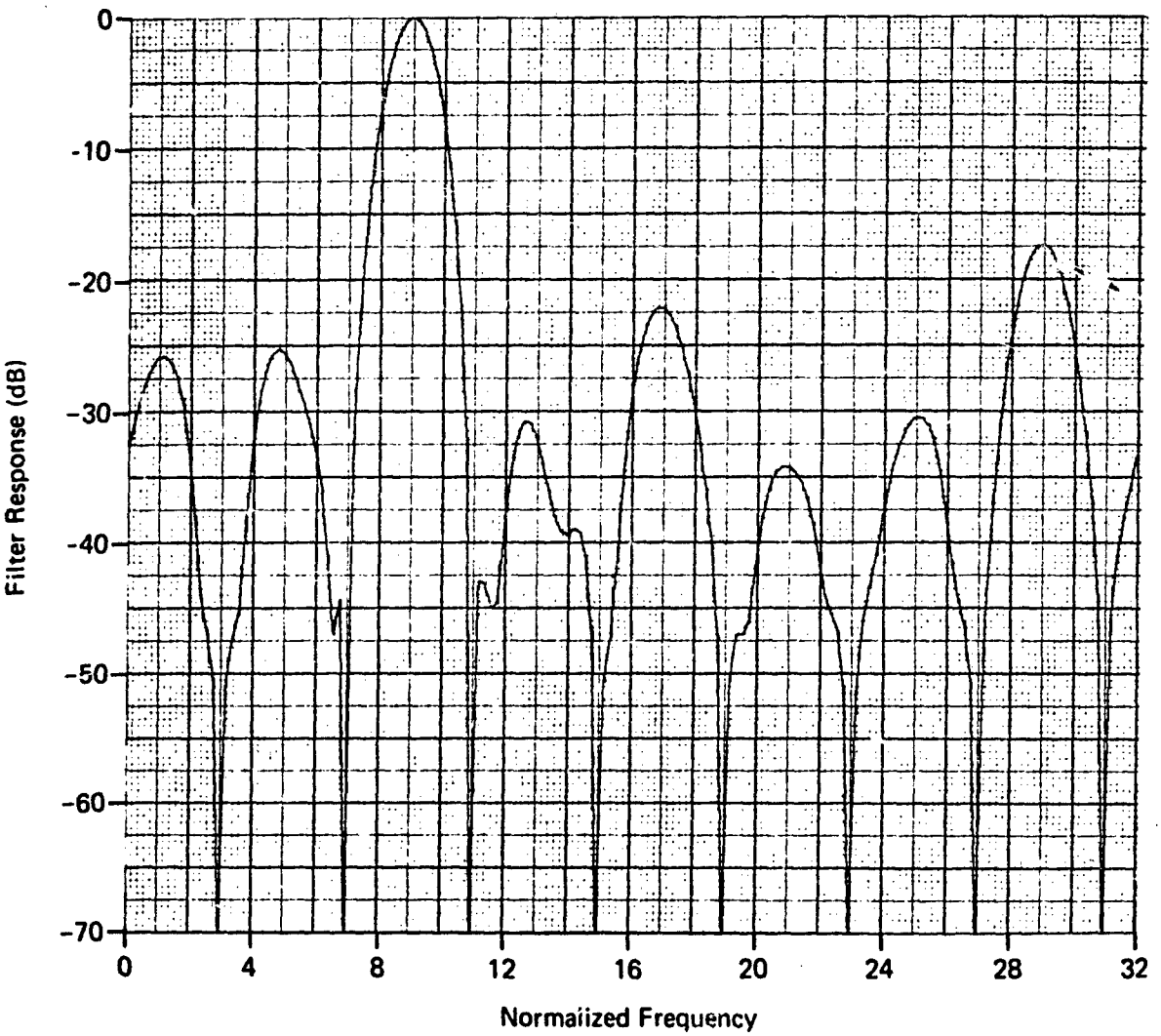

Fig. 25 Hamming Weighting 1-bit Fourier Processing; N = 32, f_0 = 9

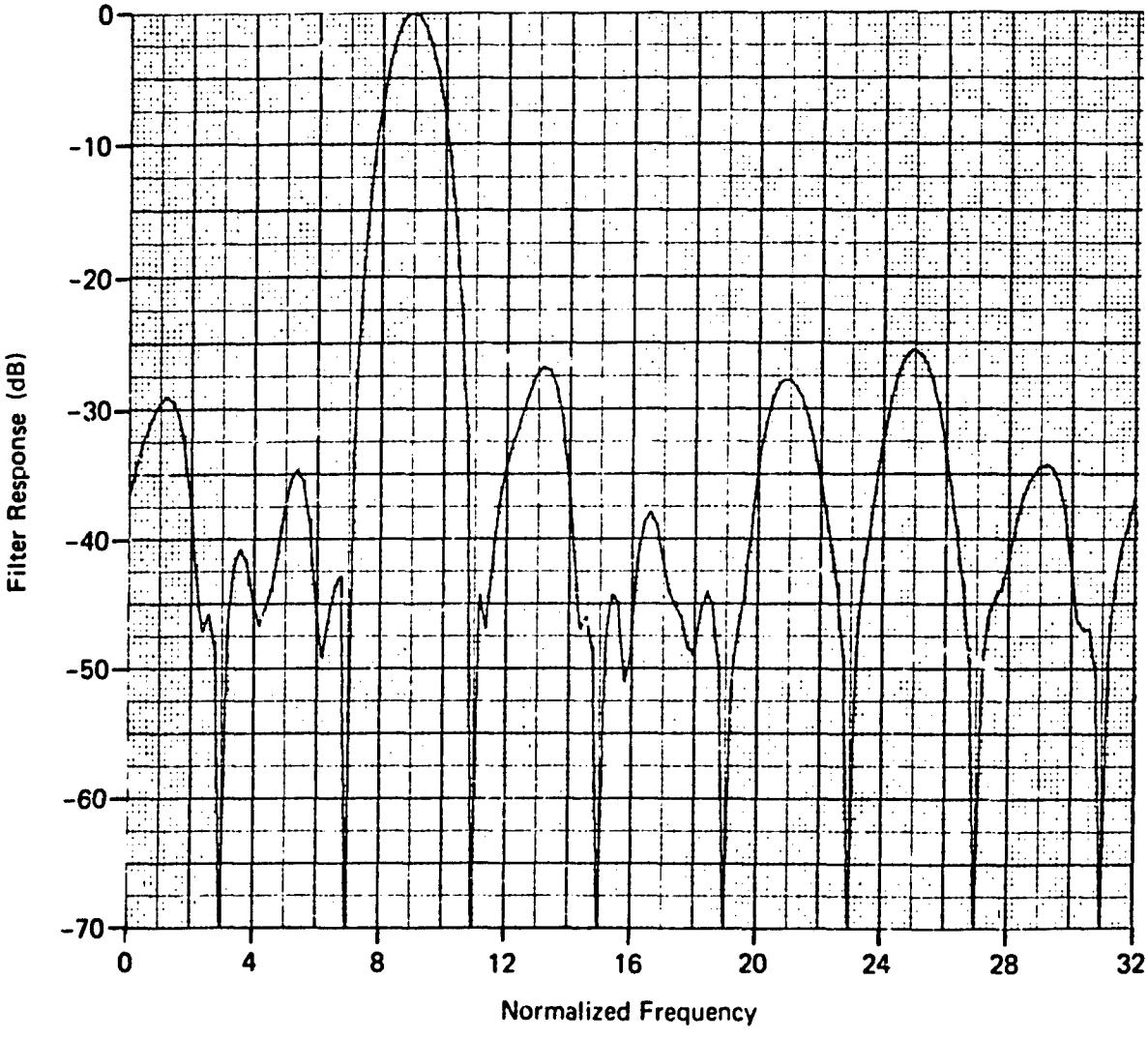

Fig. 26 Hamming Weighting 2-bit Fourier Processing; N = 32, f_0 = 9

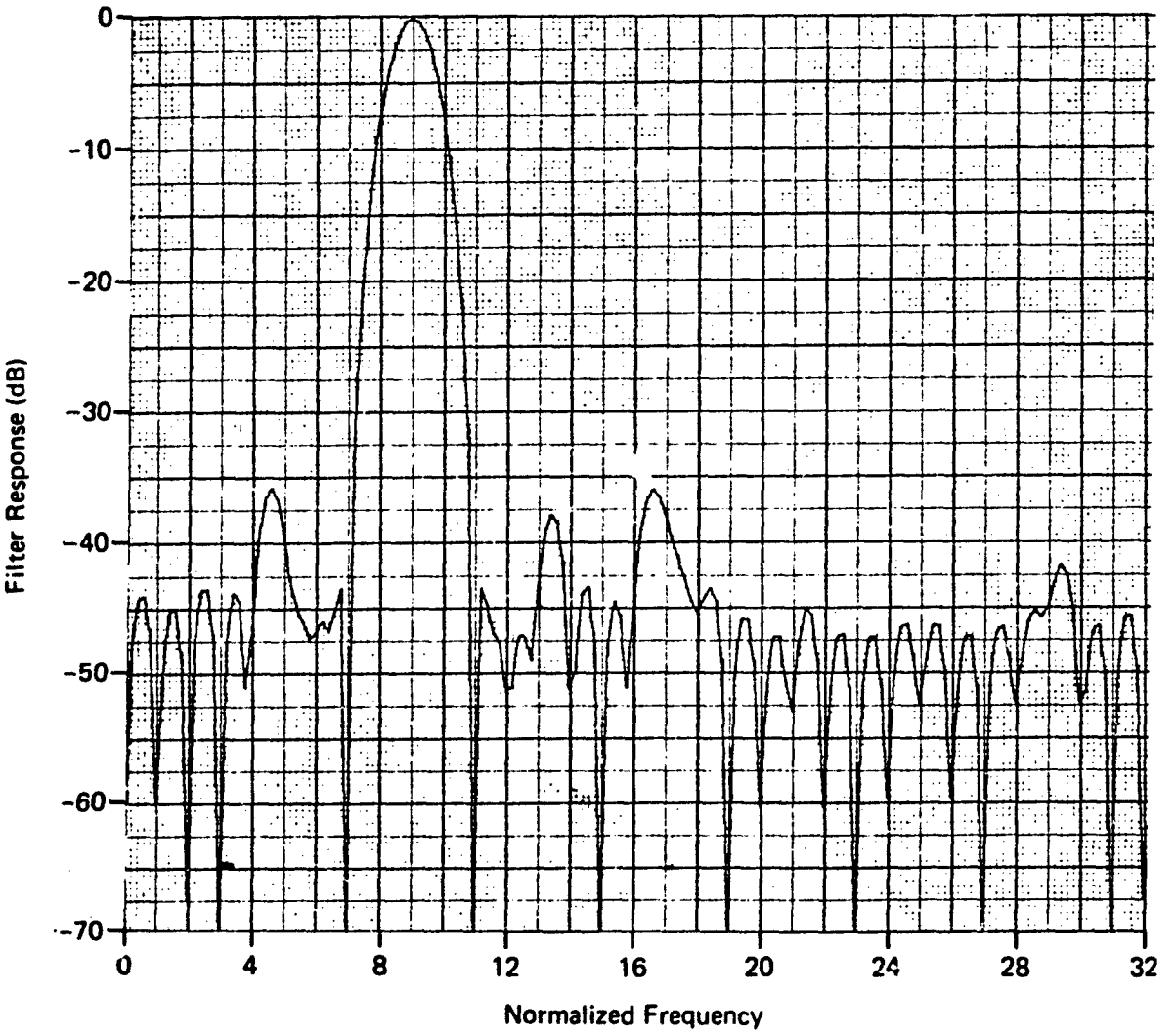

Fig. 27 Hamming Weighting 4-bit Fourier Processing; N = 32, f_0 = 9

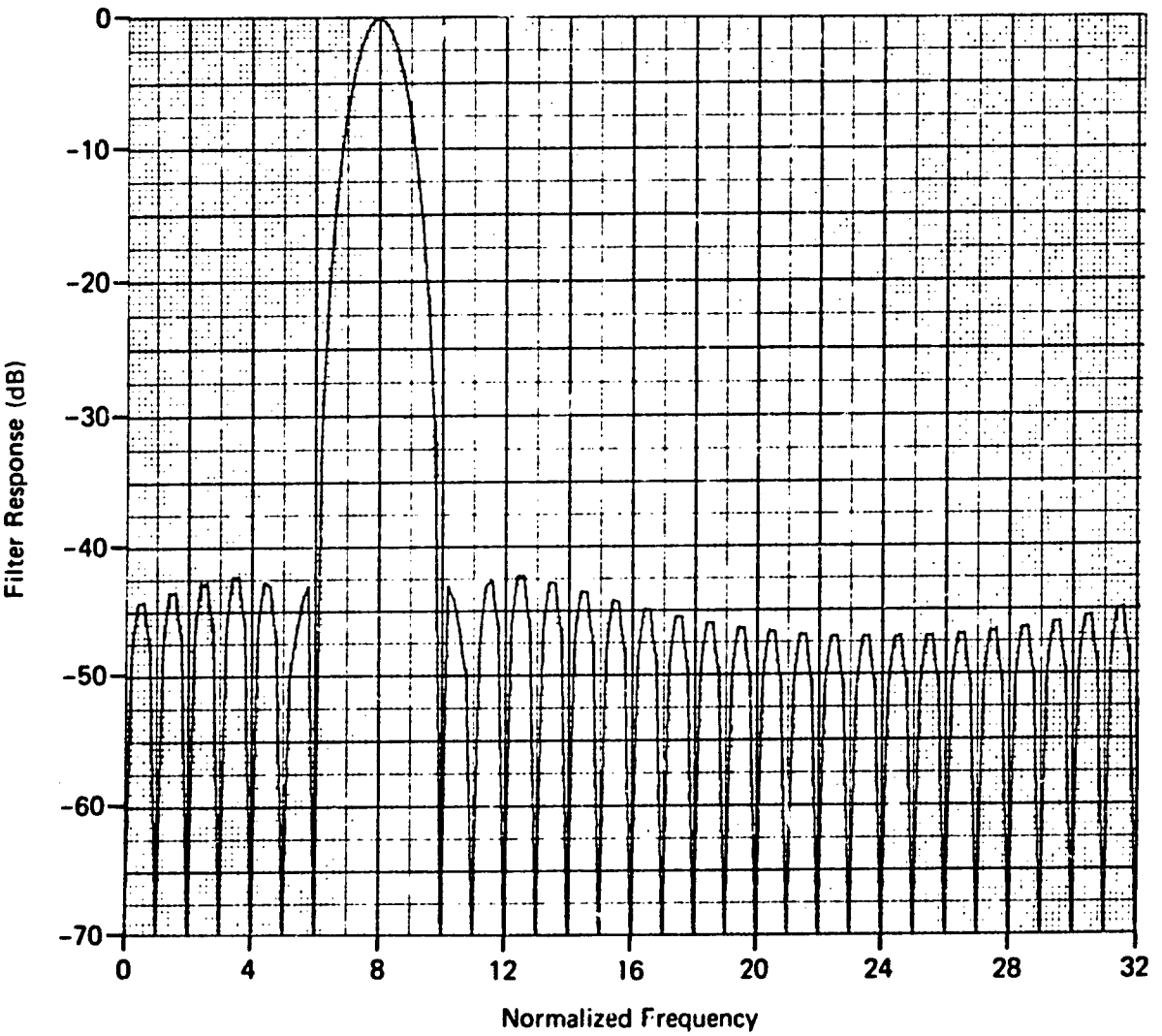

Fig. 28 Hamming Weighting 8-bit Fourier Processing; N = 32, f_0 = 9

Table 3

Peak Artifact Level Comparisons Versus Number of Amplitude Bits, 32-Point Transform

Number of Bits	Peak Level from Ref. 5 (dB)	Measured Peak Level (dB)
0	-12.0	- 9.8
1	-15.3	-15.5
2	-23.6	-25.5
4	-36.6	-36.0

4.1.4 32-Point Transform Conclusions

From the results presented above, we conclude that the Walsh transform does not seem to offer any advantages over the hard-limited Fourier transform, which has also been shown to possess various degrees of inferiority to the nonquantized DFT. The superiority of the DFT to the DWT has also been demonstrated, using a different analytical approach, by Pearl and Salzman (Ref. 4). Their approach involved an analysis of the effect of additive noise upon the ability to make an unambiguous estimate of the input signal doppler frequency, and they showed that an unambiguous estimate was possible in the absence of noise, but became rapidly more difficult as the noise level was increased. The reason for this is as follows: Suppose all the filters have sidelobes that are smaller than the filter mainlobe. Then, in the absence of noise, the frequency estimate, as mentioned earlier, is made simply by examining all the filter outputs and noting which filter has the largest output. (A minor amount of interpolation might be required if the input signal frequency was not exactly equal to a filter center frequency.) If the filters all have very low sidelobes, and a

small amount of random noise is added to the input signal, there will be small chance of making an error in frequency determination because it is unlikely that the signal plus noise vector in any sidelobe will ever be larger than the signal plus noise vector in the appropriate mainlobe. If, however, a filter has large sidelobes or artifacts, not so much noise has to be added before a good chance of making an error occurs. For example, consider a filter having a sidelobe equal in amplitude to the mainlobe. Here the chance of error is 50% even in the absence of noise! Thus the Pearl and Salzman results infer the existence of large sidelobes, but of course do not deal in detail with their location, size, or number.

4.2 256-POINT TRANSFORM

4.2.1 Introduction

For the 32-point Walsh transform it was a relatively simple matter to store the sampled values of the Walsh reference waveforms in the computer and then to generate a large data base of filter response functions. For the 256-point transform this is not a very practical procedure; nor were we able to find a simple, reliable algorithm which could be used to internally generate the appropriate Walsh function sampled values during the course of the computational cycle. Therefore, the filter response data for the Walsh transform situation were obtained only for certain of those cases where the reference signals are square waves. It will be recalled that this situation occurs when i is a power of 2, and the cases selected were $i = 4$, 8, 16, 32, and 64. The square wave sequences were obtained by adjusting the sampling instants for circular functions so as to secure only the values plus and minus unity after hard limiting. For this type of reference waveform, the term Walsh-Rademacher processing is perhaps more descriptive and will be used in the following discussion.

4.2.2 Fourier Processing, No Quantizing

Figures 29 through 31 illustrate filter transfer functions for Fourier processing with no quantizing of the reference waveforms. As in the 32-point transform case, these curves are typical of the results obtained for any of the filter center frequencies, and need no further comment except to note that the minimum sidelobe level is considerably smaller than in the 32-point transform as would be expected.

4.2.3 Walsh-Rademacher Processing

Figures 32 through 36 show typical response curves for Walsh-Rademacher processing with Hamming data weighting. Again the results are characterized by the presence of numerous artifacts. The following comments can be made on these results.

1. The peak artifact level was -7.6 dB.

2. The total number of artifacts exceeding -30 dB is 26, or an average of 6.5 per filter (the $i = 64$ filter has no artifacts – see No. 3 below). The median artifact level was -19.4 dB.

3. For the filter having a center frequency of 64, there were no artifacts. This is exactly analogous to the situation where the center frequency in the 32-point transform was eight.

4. Although the number of artifacts decreased with increasing i, this would probably not be true in general, as illustrated by the 32-point transform results.

5. A comparison of Fig. 32 with Fig. 7, and Fig. 33 with Fig. 10, illustrates the effects of changing the number of points in a Walsh-Rademacher transform upon filter response.

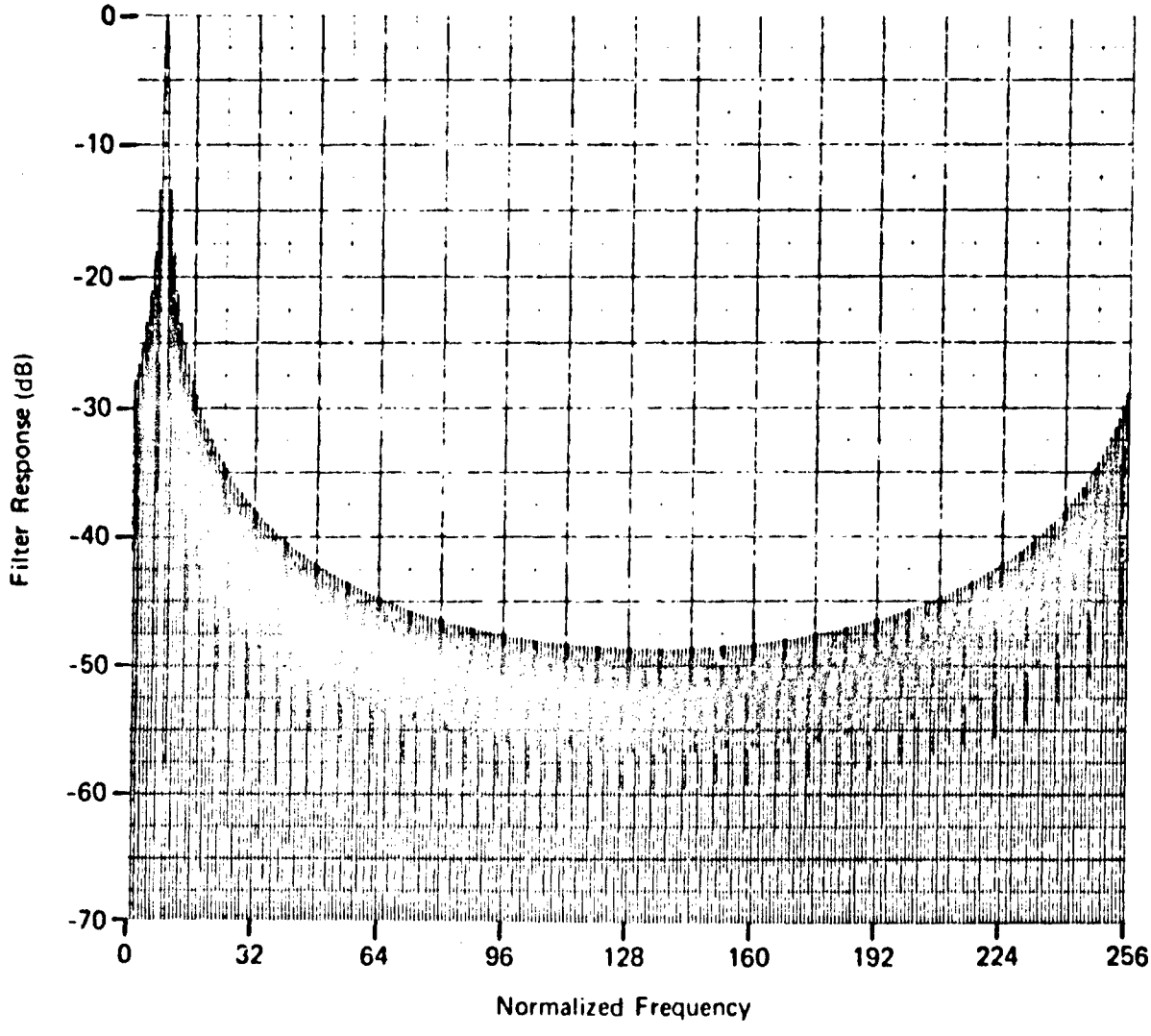

Fig. 29 Uniform Weighting Fourier Processing; N = 256, f_0 = 8

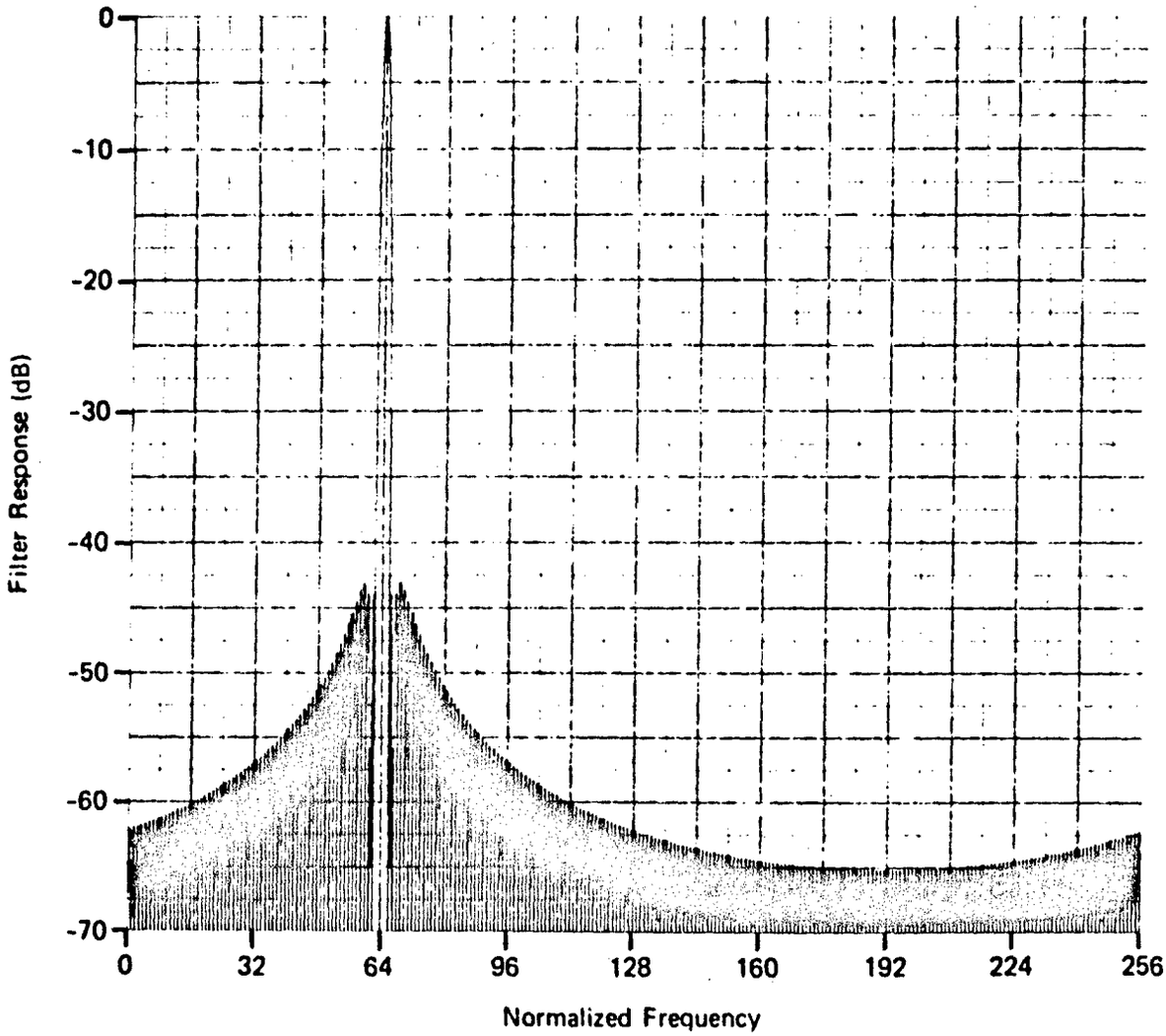

Fig. 30 Hamming Weighting Fourier Processing; N = 256, f_0 = 64

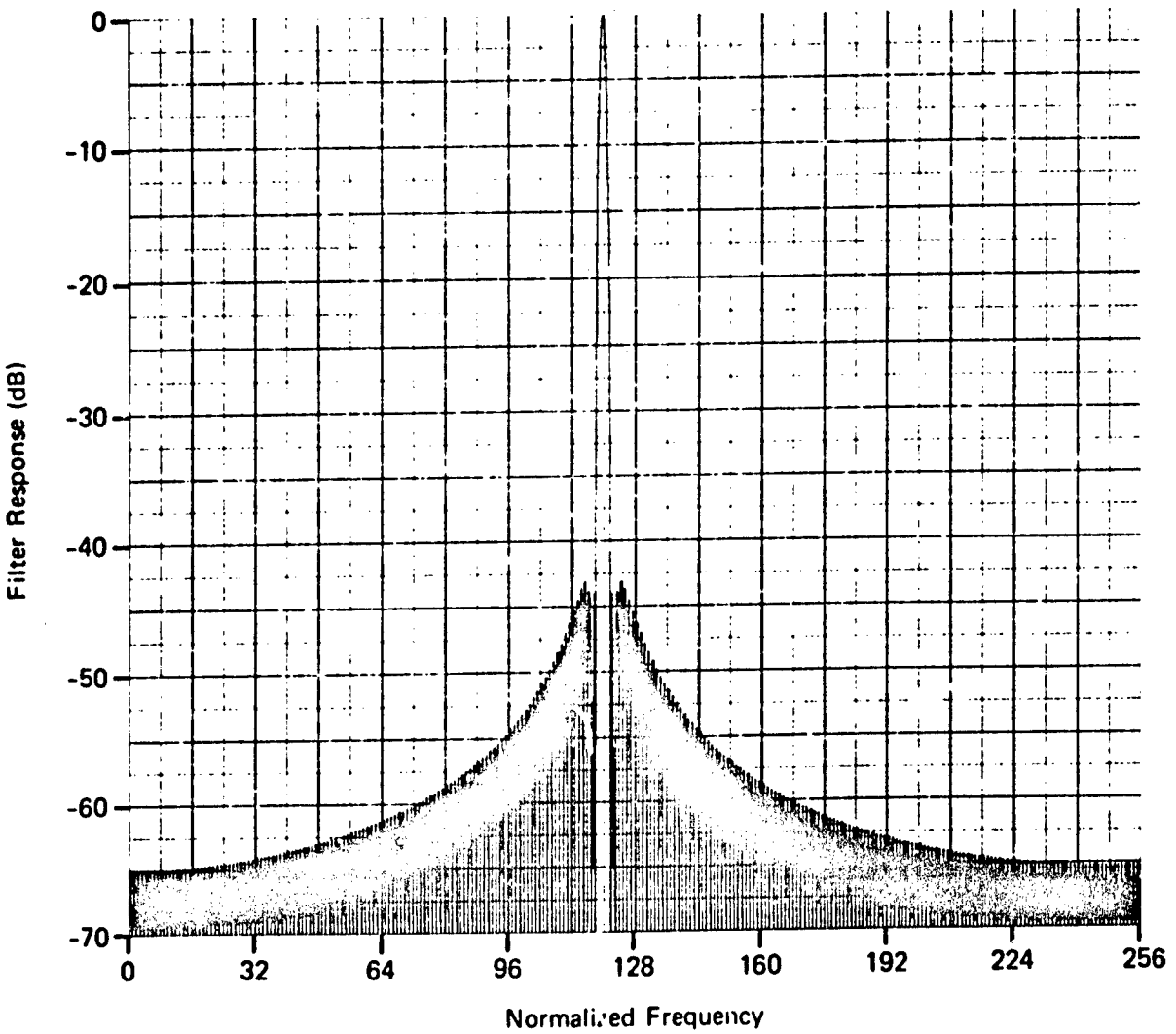

Fig. 31 Hamming Weighting Fourier Processing; N = 256, f_0 = 120

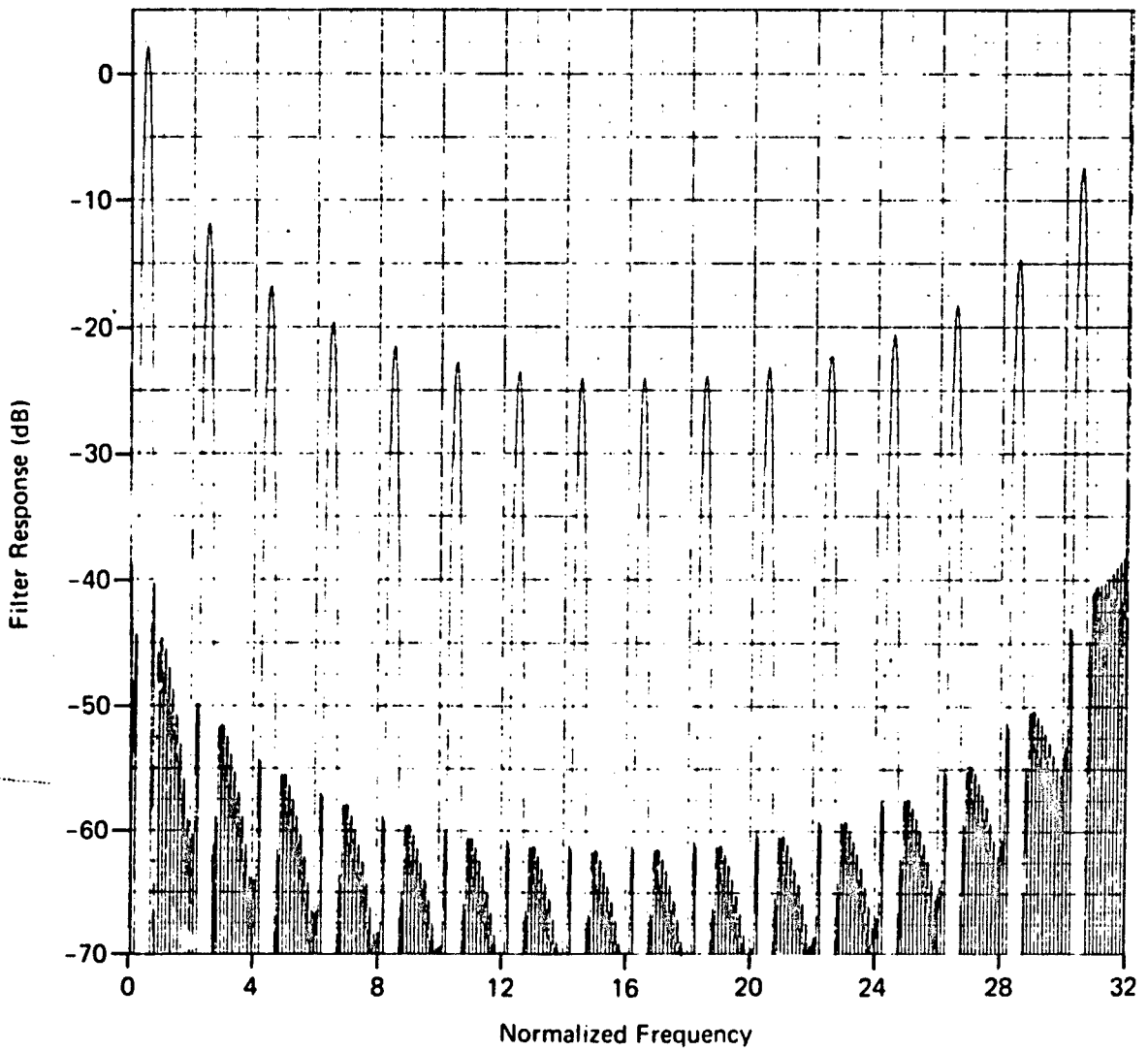

Fig. 32 Hamming Weighting Walsh Processing; N = 256, f_0 = 4

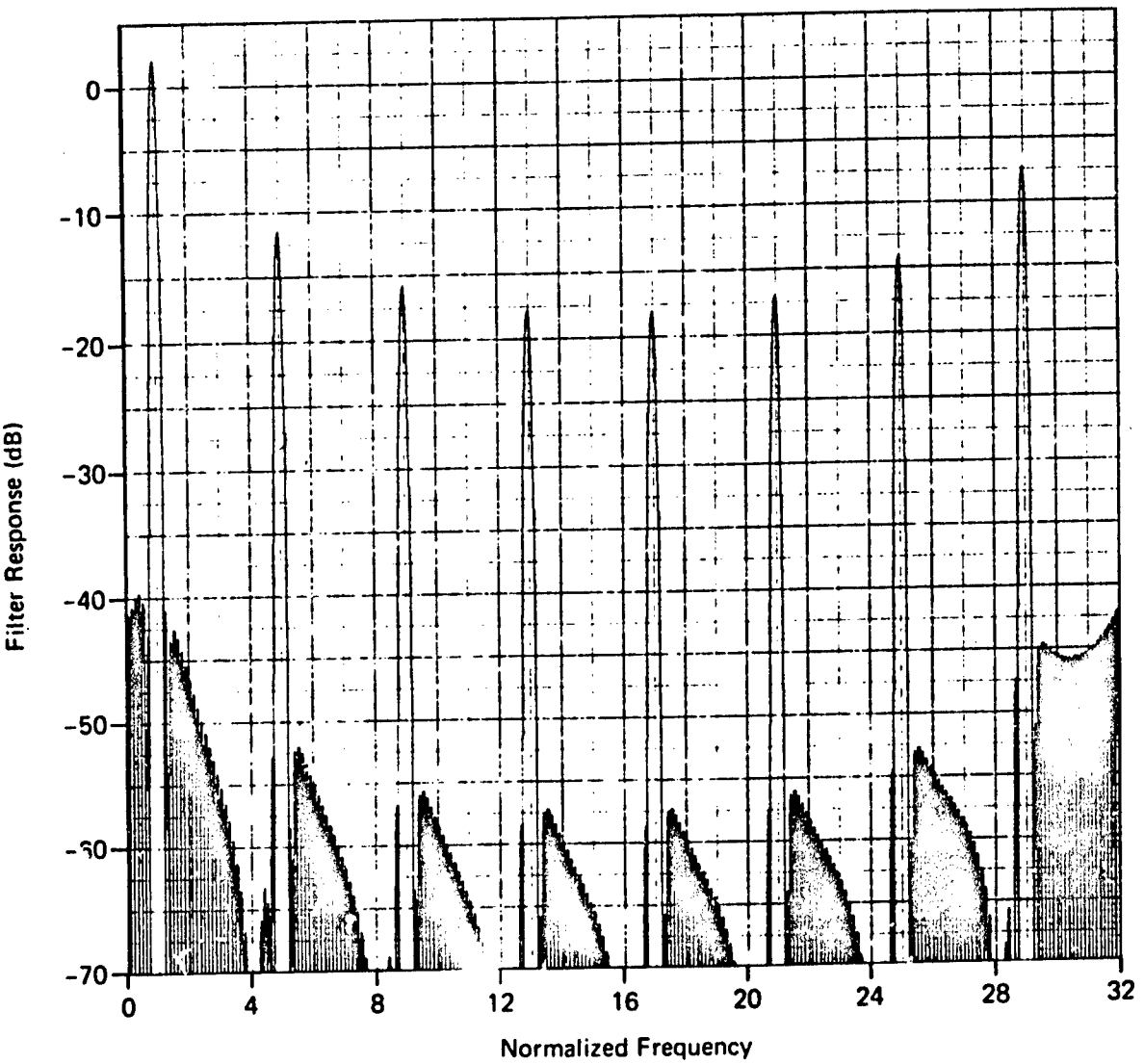

Fig. 33 Hamming Weighting Walsh Processing; N = 256, f_0 = 8

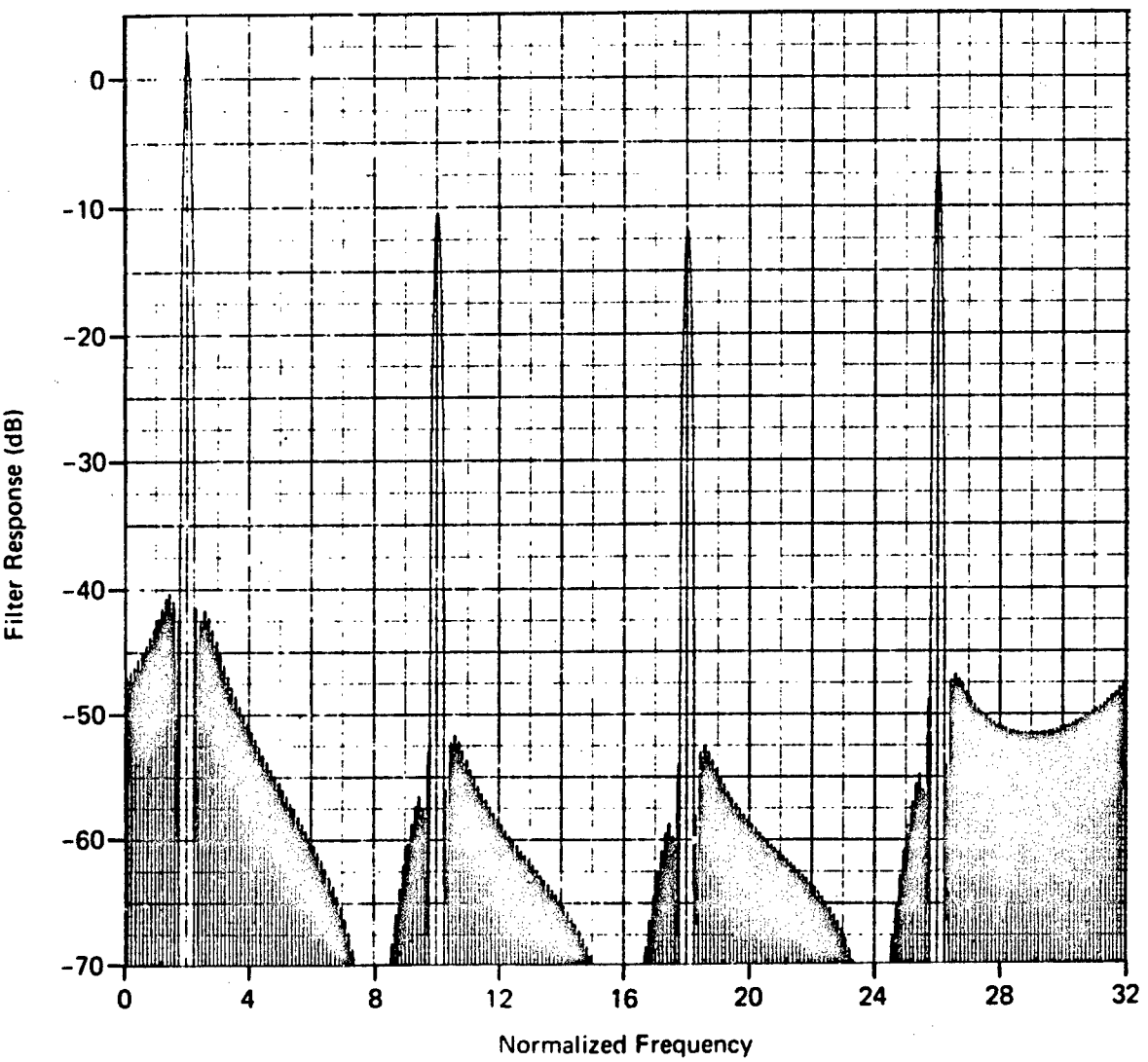

Fig. 34 Hamming Weighting Walsh Processing; N = 256, f_0 = 16

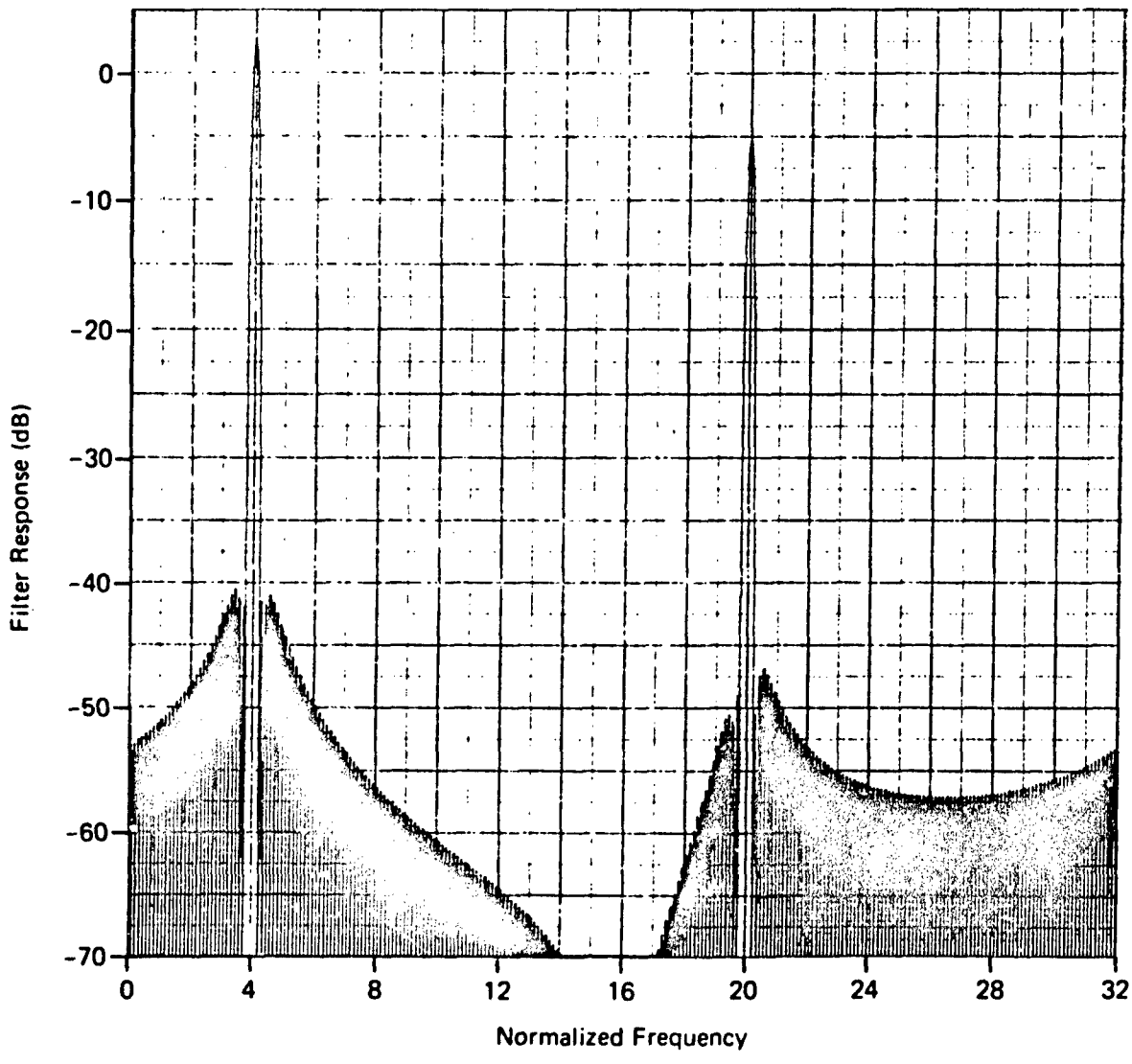

Fig. 35 Hamming Weighting Walsh Processing; N = 256, f_0 = 32

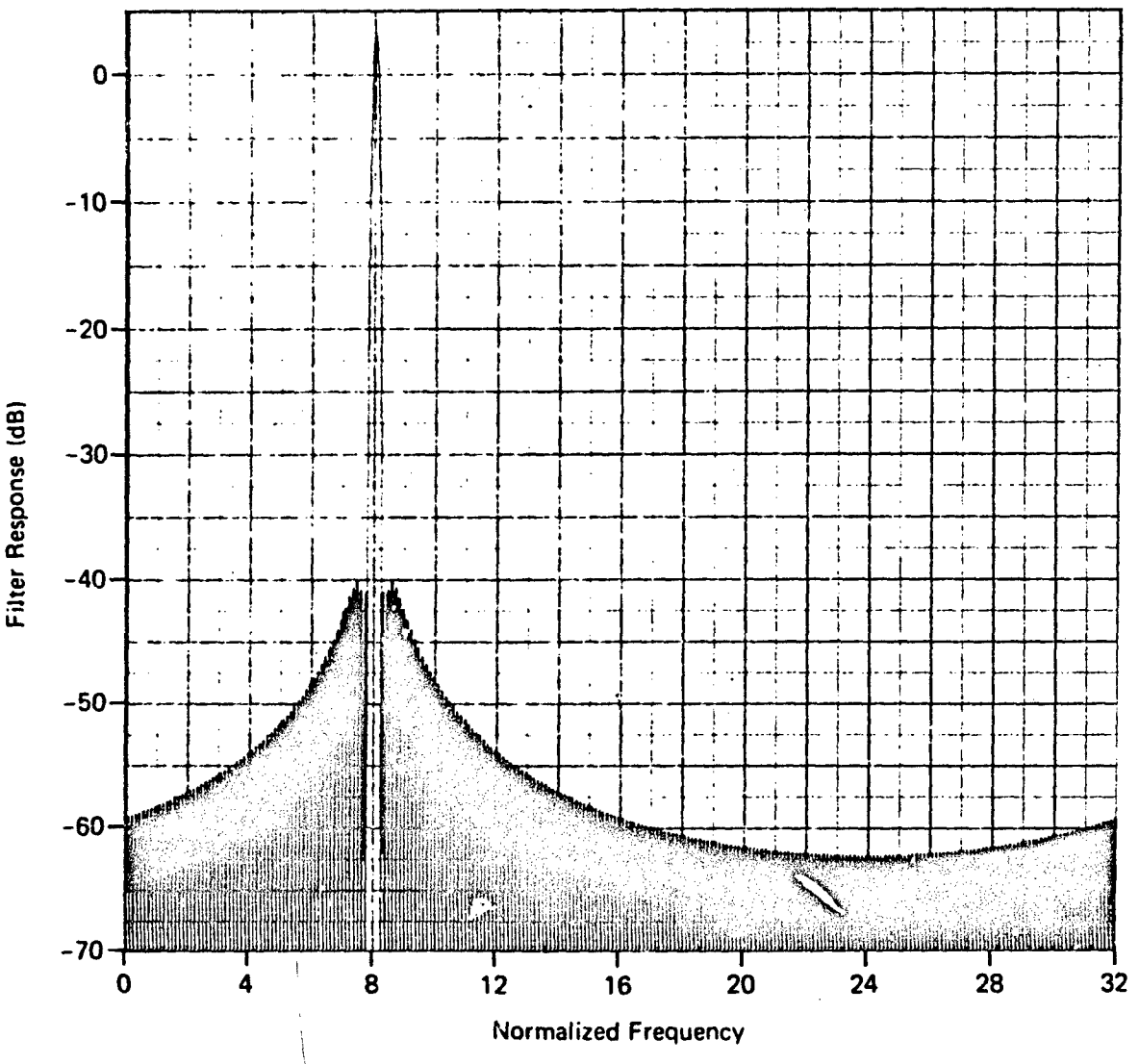

Fig. 36 Hamming Weighting Walsh Processing; N = 256, f_0 = 64

6. In certain instances the presence of an artifact was accompanied by a pronounced lowering of the nearby interartifact sidelobe level. This suggests that a suitably chosen randomization of the axis crossing times of the reference waveforms might be used to reduce the artifact levels, but this was not investigated.

7. There was no observed tendency for artifacts to avoid the regions around $f = 0$ and $f = 256$.

Although we have obtained filter response data for less than 4% of the 128 possible Walsh transform response curves, these results (when considered together with the more extensive 32-point transform data) suggest strongly that the artifact problem would be quite severe in an unacceptably high percentage of the other 256-point Walsh transform filter response curves.

4.2.4 Quantized Fourier Processing

Filter response data were also obtained for the values of i equal to 4, 6, 8, 12, 16, 25, 32, 45, 55, 120, and 124 for the cases where the amplitude levels of the reference waveforms were quantized to 1, 2, 4, and 8 bits and Hamming data weighting was used. Because of the large number of near-in artifacts present in some filters, we can say, for the 8-bit case, only that the peak artifact level never exceeded the artifact-free sidelobe level by more than 5 dB. For the other cases, the peak levels are compared with the peak levels of Ref. 5 in Table 4. The agreement of the results with those in Table 3, and with Ref. 5 are quite remarkable. Figures 37 through 45 illustrate typical filter response curves for the 4-bit situation, while Fig. 46 is a typical response curve for 8-bit quantization.

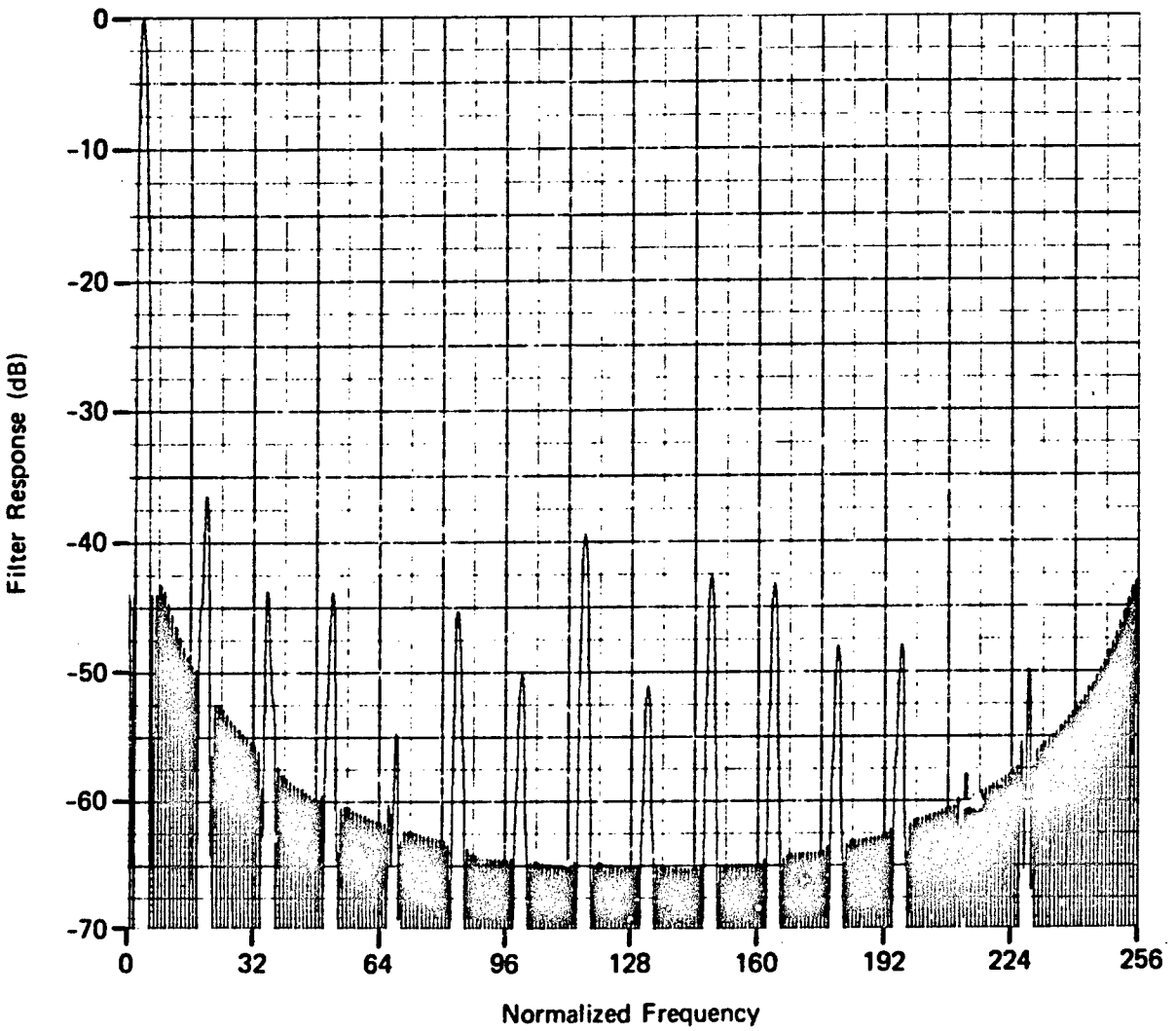

Fig. 37 Hamming Weighting 4-bit Fourier Processing; N = 256, $f_0 = 4$

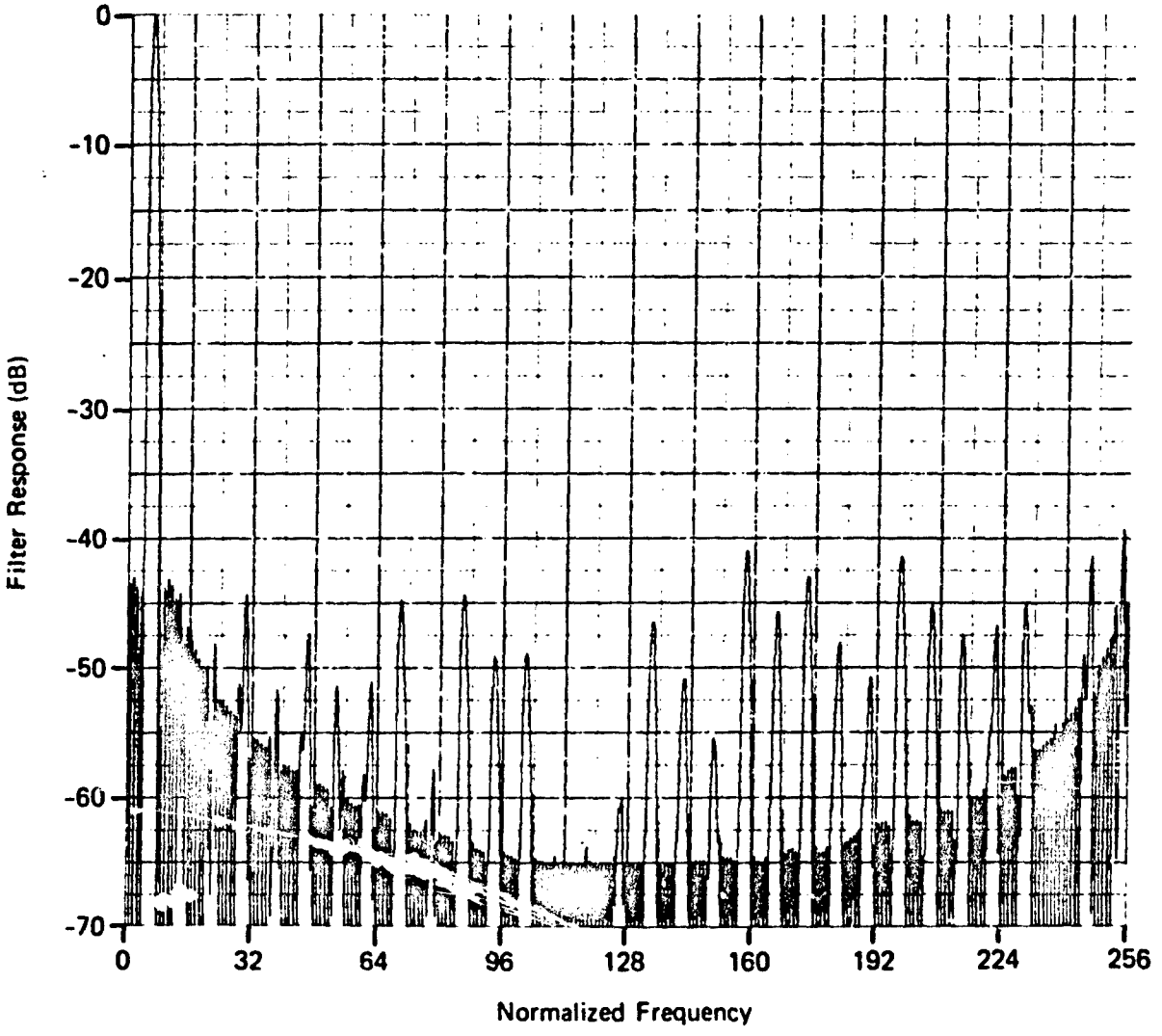

Fig. 38 Hamming Weighting 4-bit Fourier Processing; N = 256, f_0 = 6

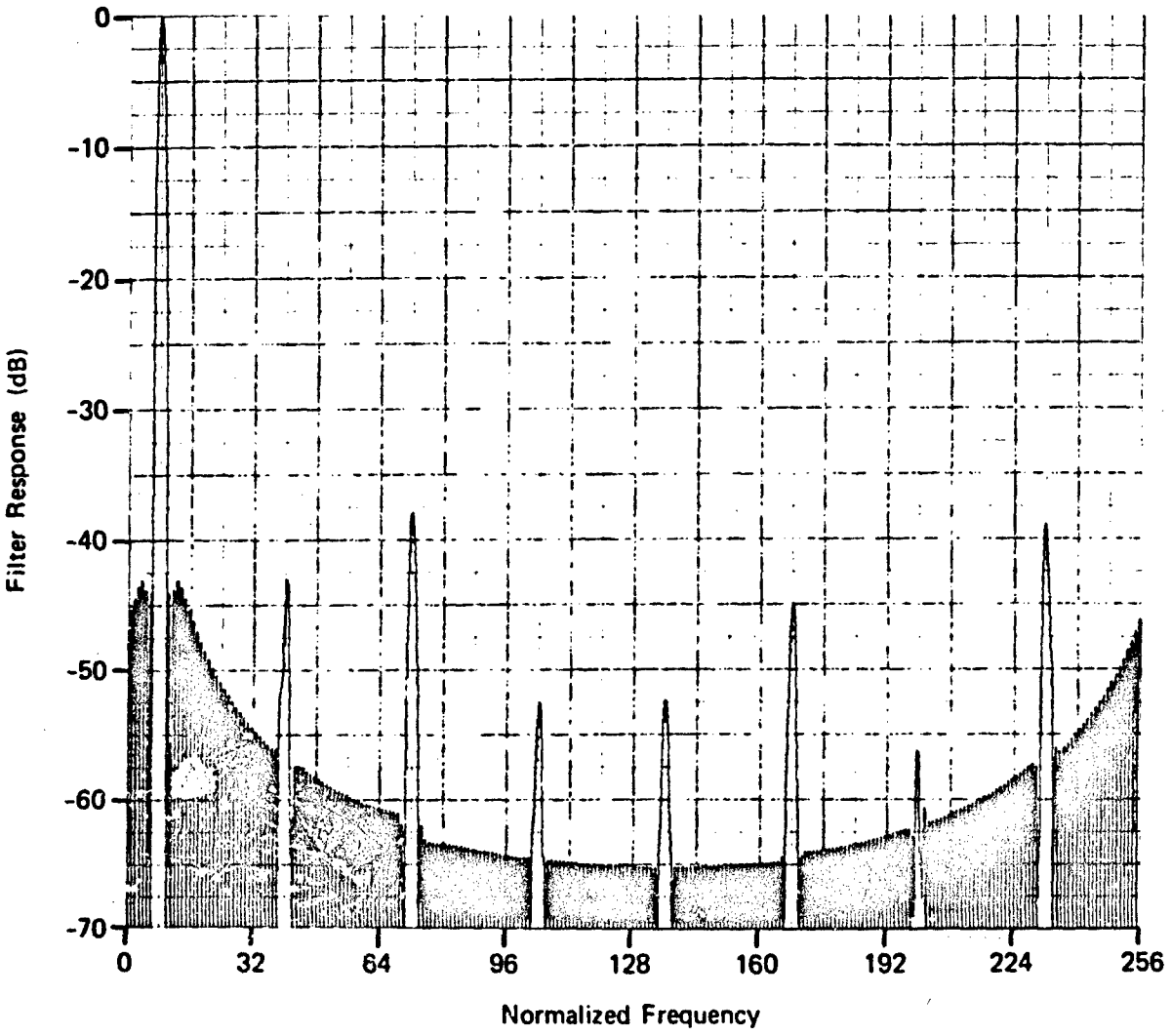

Fig. 39 Hamming Weighting 4-bit Fourier Processing; N = 256, f_0 = 8

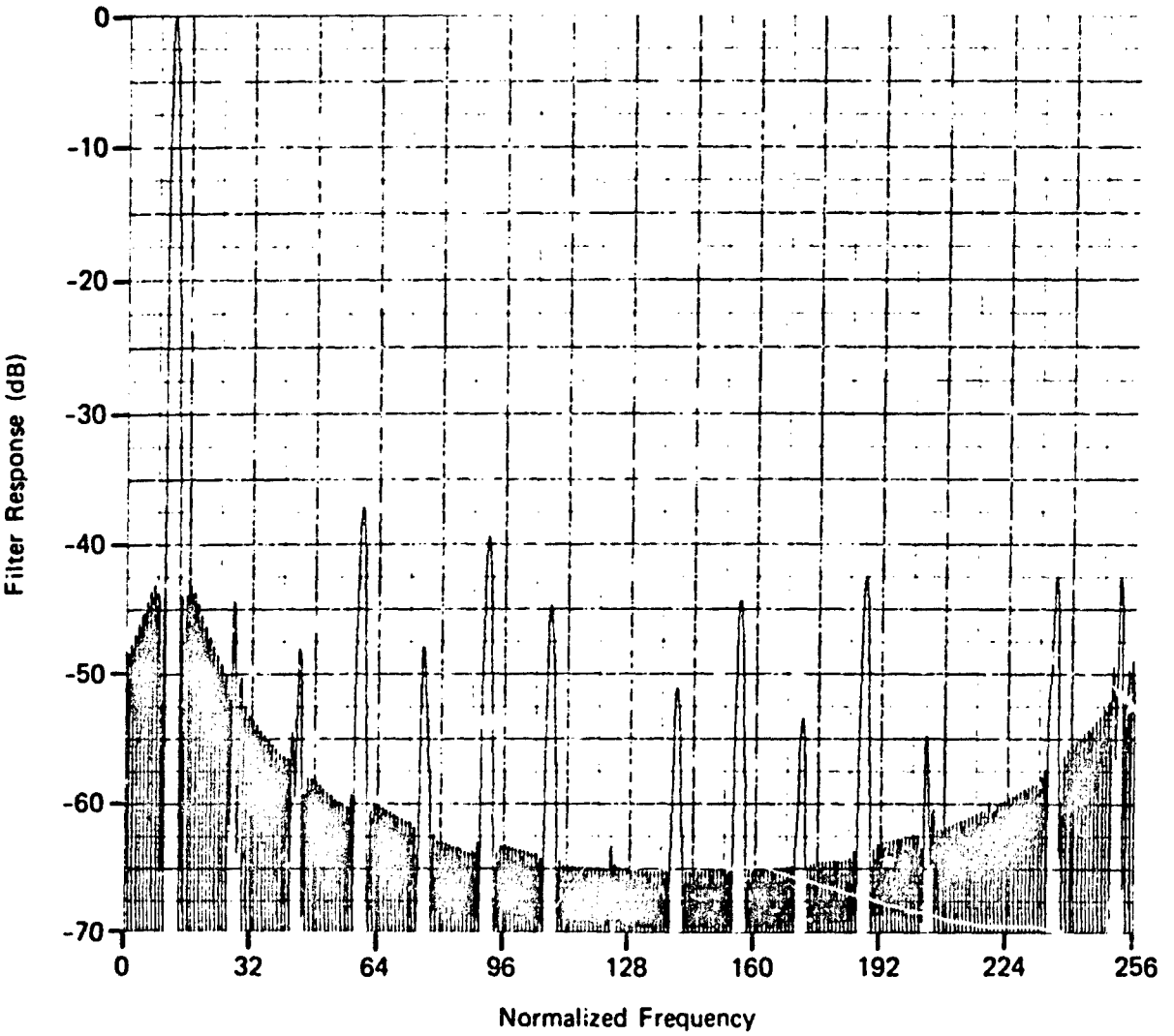

Fig. 40 Hamming Weighting 4-bit Fourier Processing; N = 256, f_0 = 12

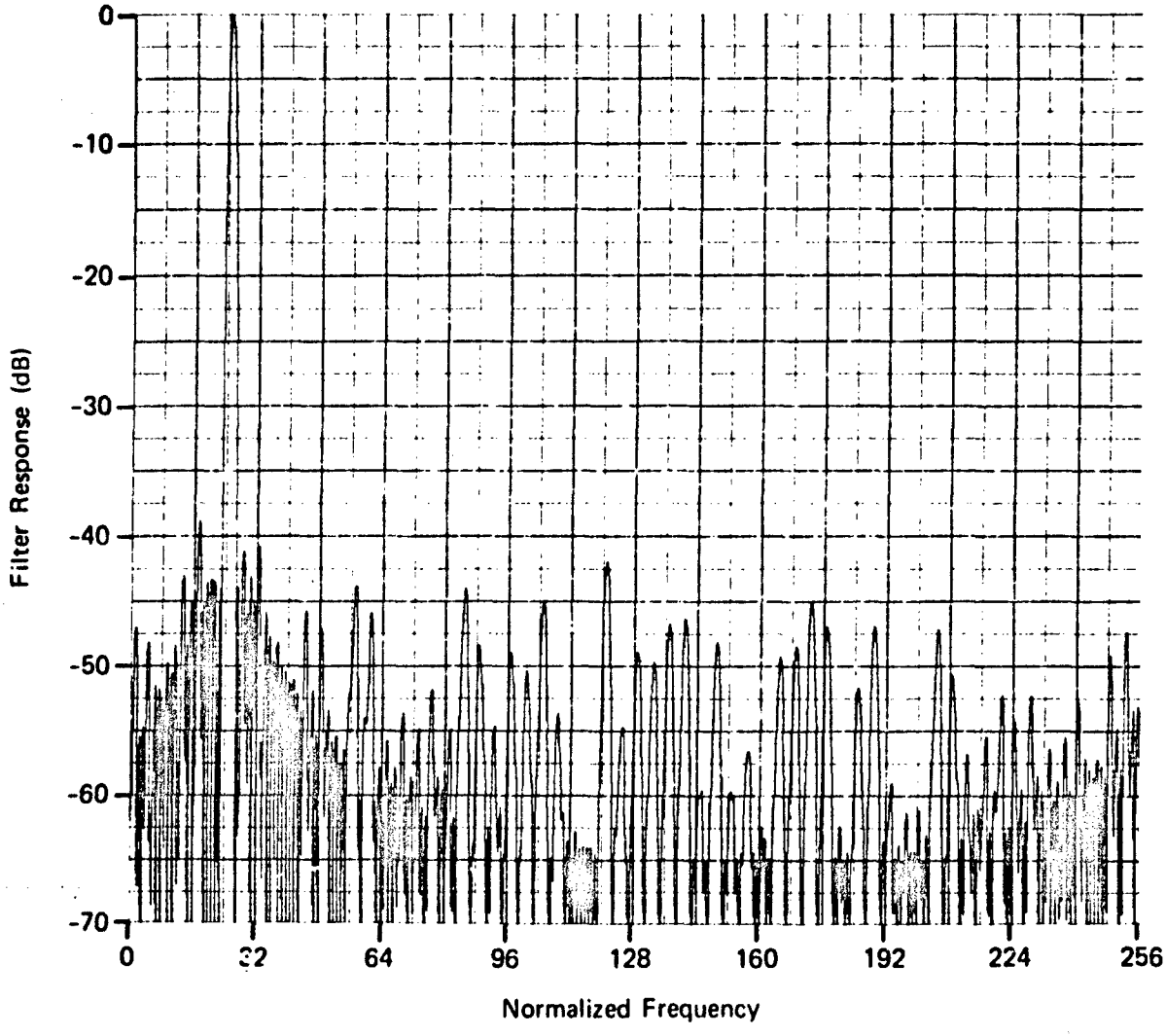

Fig. 41 Hamming Weighting 4-bit Fourier Processing; N = 256, f_0 = 25

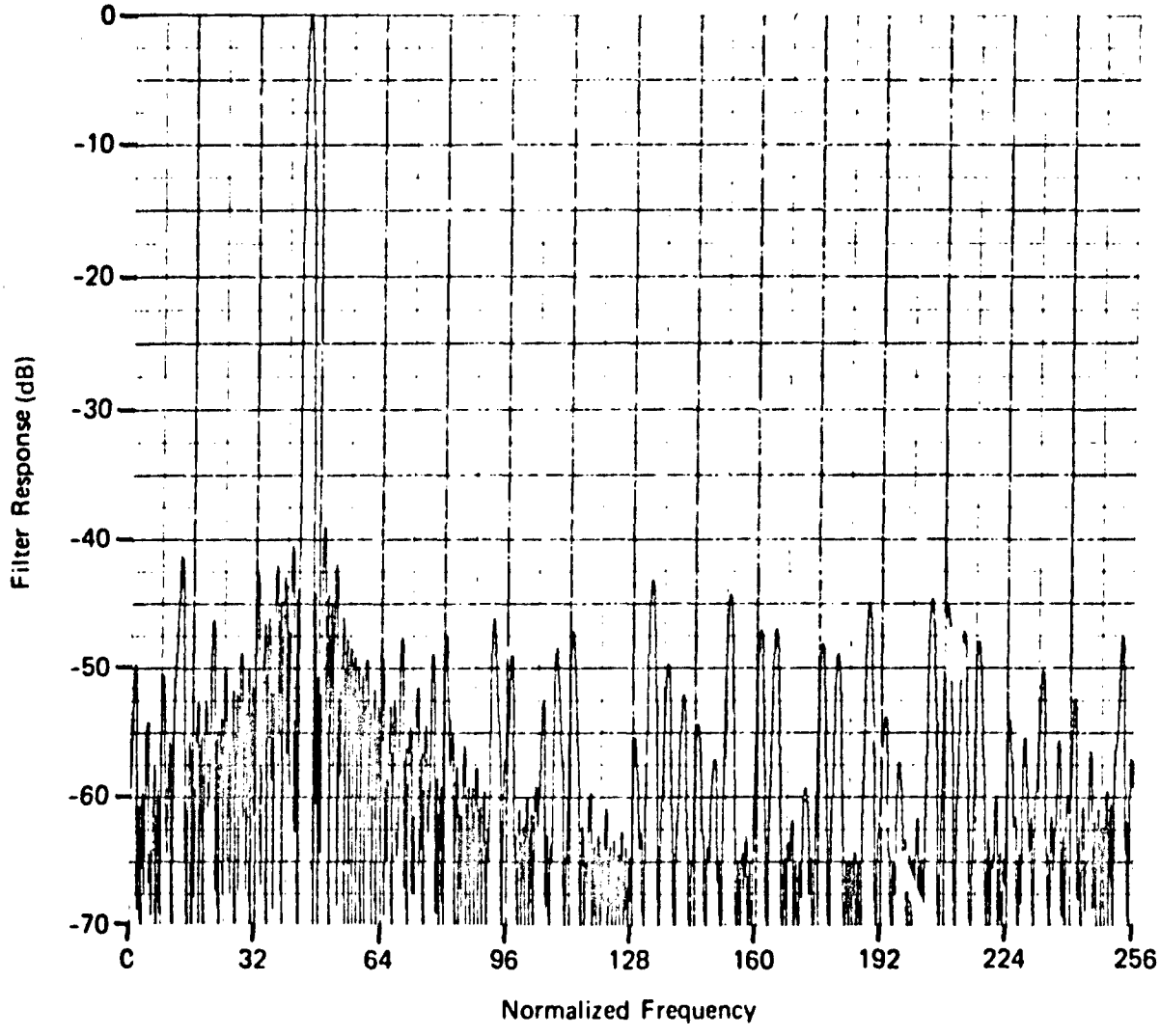

Fig. 42 Hamming Weighting 4-bit Fourier Processing; N = 256, f_0 = 45

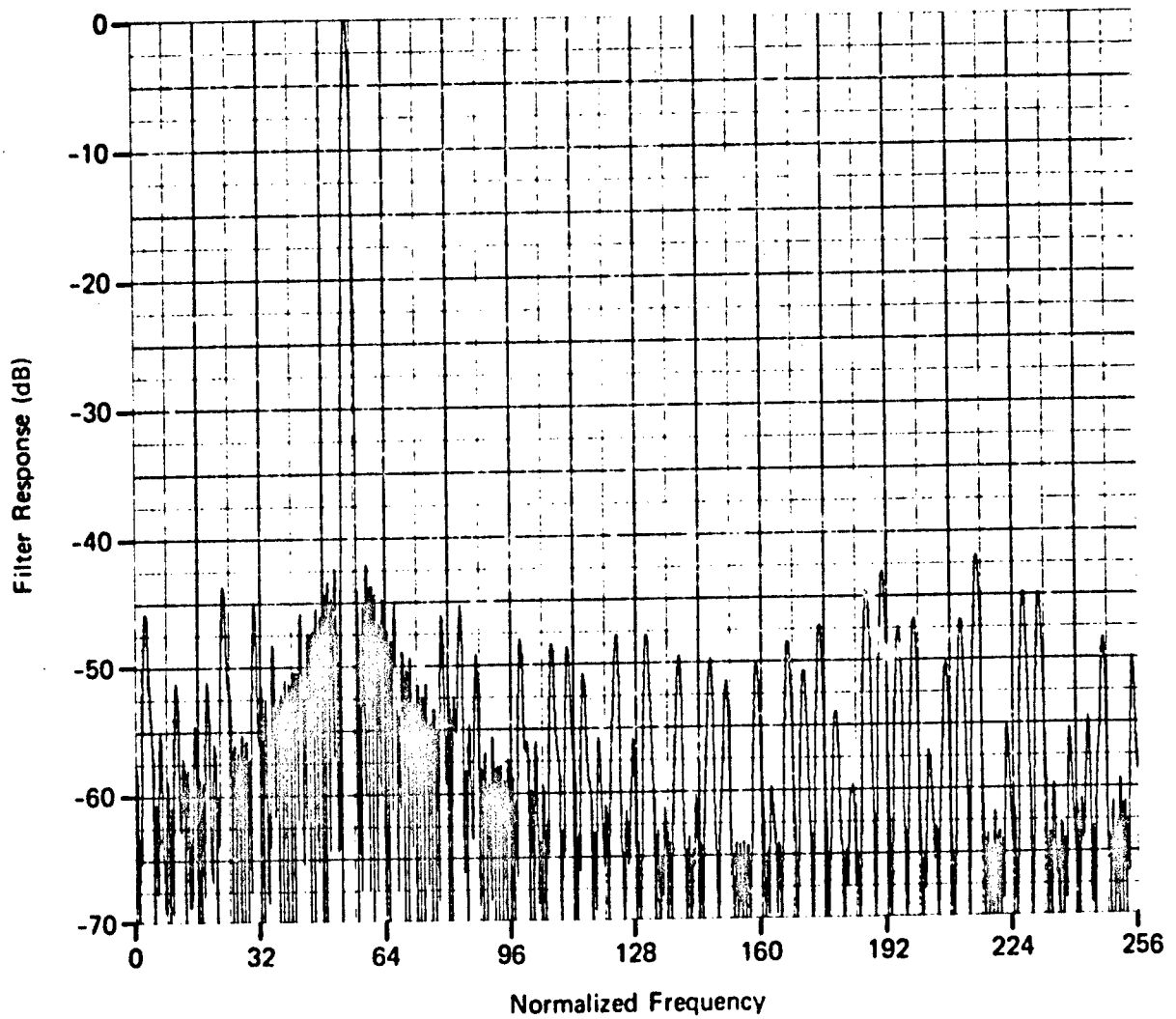

Fig. 43 Hamming Weighting 4-bit Fourier Processing; N = 256, f_0 = 55

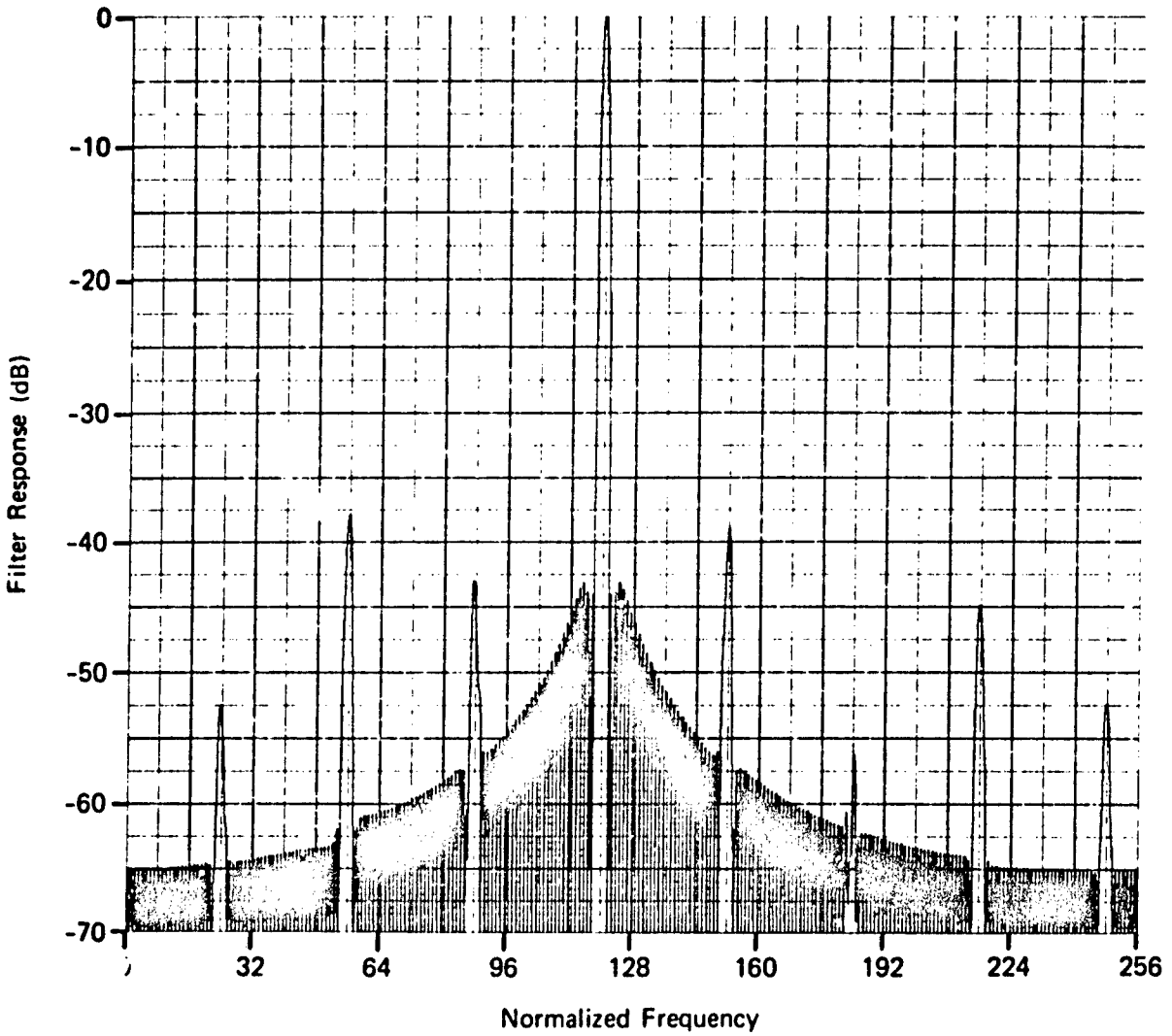

Fig. 44 Hamming Weighting 4-bit Fourier Processing; N = 256, f_0 = 120

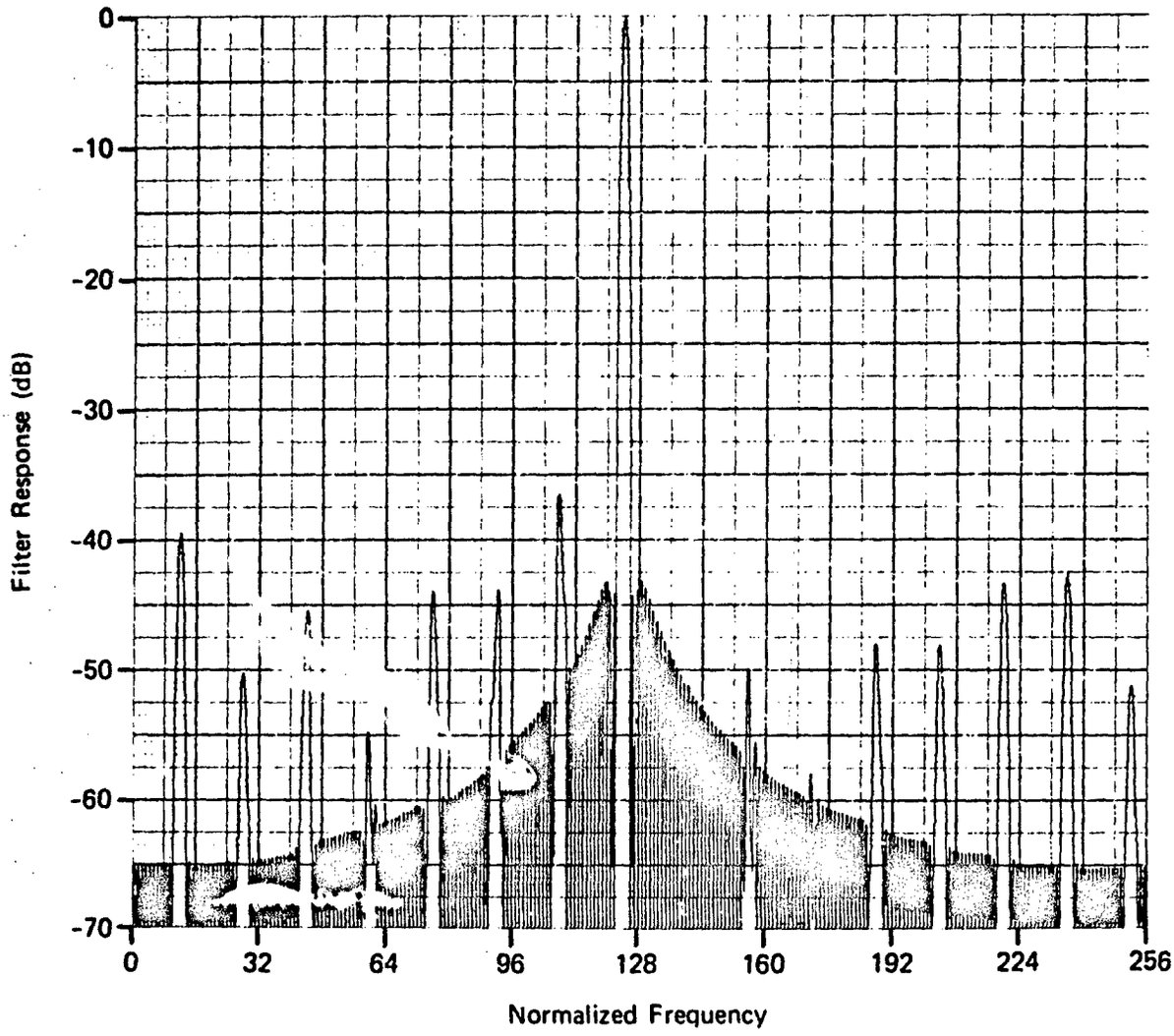

Fig. 45 Hamming Weighting 4-bit Fourier Processing; N = 256, f_0 = 124

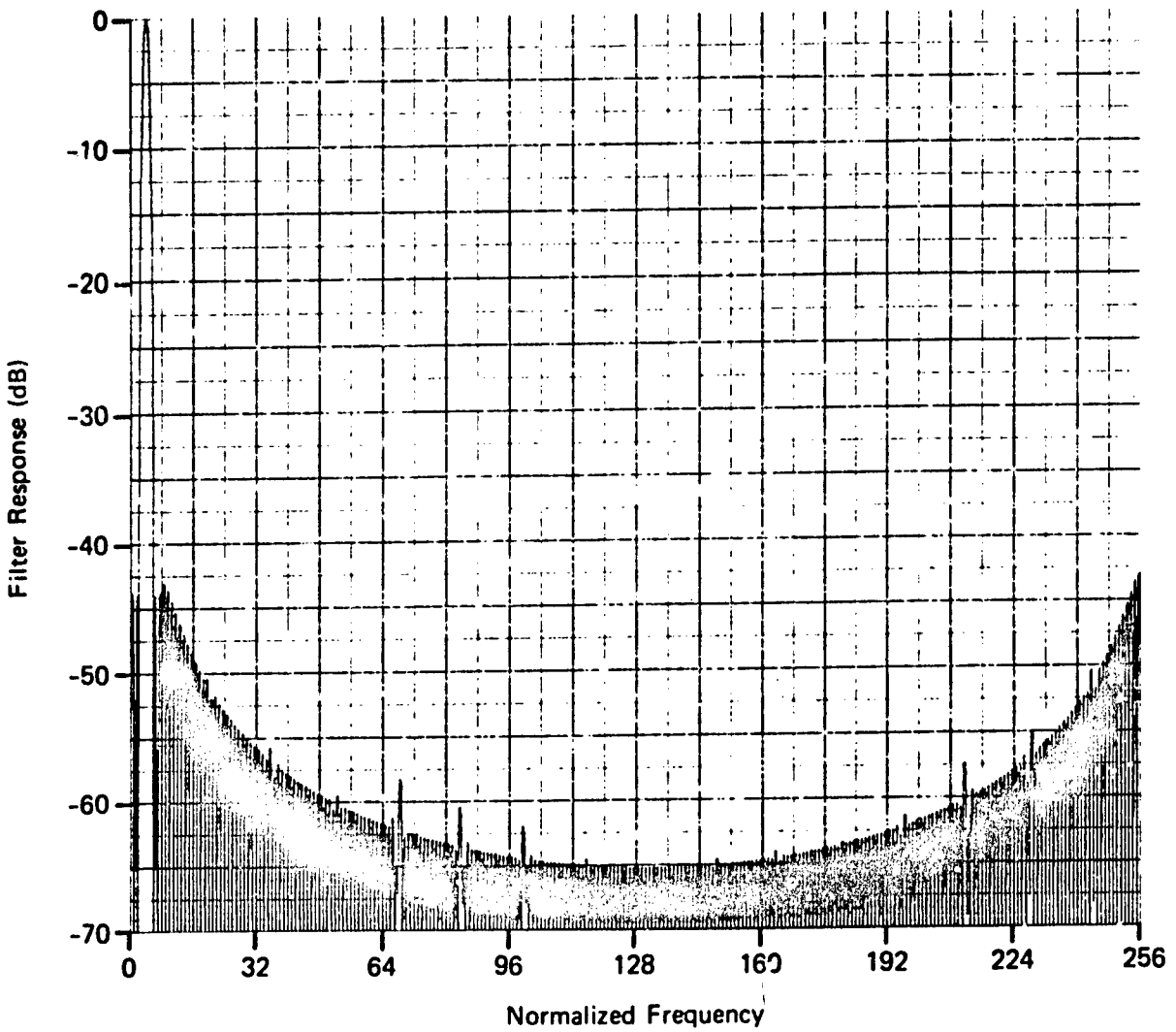

Fig. 46 Hamming Weighting 8-bit Fourier Processing; N = 256, $f_0 = 4$

Table 4

Peak Artifact Level Comparisons versus Number of Amplitude Bits, 256-Point Transform

Number of Bits	Peak Level from Ref. 5 (dB)	Measured Peak Level (dB)
1	-15.3	-15.0
2	-23.6	-25.5
4	-36.6	-36.5

4.2.5 256-Point Transform Conclusions

The computations we have made in the case of the 256-point Walsh-Rademacher and Fourier transforms show, as did also the 32-point computations, that the appearance of numerous artifacts is the price one must pay if the amplitudes of the reference waveforms are represented by only a small number of bits. While such artifacts may not pose a problem in certain applications of Walsh or heavily quantized Fourier transforms, they would certainly hinder the radar clutter suppression and target ambiguity resolution processes.

REFERENCES

1. H. F. Harmuth, Transmission of Information by Orthogonal Functions, Springer-Verlag, First Ed. 1969, Second Ed. 1972.

2. N. M. Blachman, "Sinusoids versus Walsh Functions," Proc. IEEE, Vol. 62, March 1974, pp. 346-354.

3. J. Salzman, Discrete Transform Methods in Adaptive Radar Detection, M. S. Thesis, UCLA, 1973.

4. J. Pearl and J. Salzman, "Comparison of Fourier and Walsh Transforms in Radar Signal Processing," Proc. 1973 Symp. on the Applications of Walsh Functions.

5. D. W. Tufts, H. S. Hersey, and W. E. Mosier, "Effects of FFT Coefficient Quantization on Bin Frequency Response," Proc. IEEE, January 1972, pp. 146-147.

6. D. W. Tufts, D. W. Rorabacher, and W. E. Mosier, "Designing Simple, Effective Digital Filters," IEEE Trans. Audio and Electroacoustics, Vol. AU-18, June 1970, pp. 142-158.

7. R. A. Meyer, D. G. Grant, and J. L. Queen, A Digital-Optical Hybrid Correlator, APL/JHU TG 1193A, September 1972

8. W. H. Zinger and R. F. Platte, personal communication.

9. E. E. Nathanson, Radar Design Principles, Section 14.8, McGraw Hill, 1969.

10. R. B. Blackman and J. W. Tukey, The Measurement of Power Spectra, Dover Publications, 1959.

BIBLIOGRAPHY

1. J. L. Walsh, "A Closed Set of Normal Orthogonal Functions," Amer. J. Math., Vol. 45, 1923, pp. 5-24.

2. J. E. Whelchel and D. F. Guinn, "The Fast Fourier-Hadamard Transform and Its Use in Signal Representation and Classification," 1968 EASCON Convention Record, pp. 561-573.

3. W. K. Pratt, J. Kane, and H. C. Andrews, "Hadamard Transform Image Coding," Proc. IEEE, Vol. 57, January 1969, pp. 58-67.

4. H. F. Harmuth, "Applications of Walsh Functions in Communications," IEEE Spectrum, November 1969, pp. 82-91.

5. H. F. Harmuth, "Sequency Filters Based on Walsh Functions," IEEE Trans. EMC, June 1968, pp. 293-295.

6. Proceedings of the 1970 Symposium on the Applications of Walsh Functions, Washington, D. C., AD 707431.

7. Proceedings of the 1971 Symposium on the Applications of Walsh Functions, Washington, D. C., AD 727000.

8. Proceedings of the 1972 Symposium on the Applications of Walsh Functions, Washington, D. C., AD 744650.

9. Proceedings of the 1973 Symposium on the Applications of Walsh Functions, Washington, D. C., AD 763000.

Preceding page blank

BIBLIOGRAPHY (Cont'd.)

10. Proceedings of the 1974 Symposium on the Applications of Walsh Functions, Washington, D. C.

11. N. Ahmed and K. R. Rao, "Transform Properties of Walsh Functions," 1971 Fall IEEE Conference Proceedings, pp. 378-382.

12. K. G. Beauchamp, "The Walsh Power Spectrum - Its Derivation and Use," Proc. 1971 NEC, pp. 377-382.

13. W. K. Pratt, "Digital Transforms," 1973 NEREM Convention Record, pp. 11-20.

14. J. Pearl, "Basis – Restricted Transformations and Performance Measures for Spectral Representations," IEEE Trans. Info.Theory, November 1971, pp. 751-752.

15. J. Pearl, H. C. Andrews, and W. K. Pratt, "Performance Measures for Transform Data Coding," IEEE Trans. on Communications, June 1972, pp. 411-415.

16. J. E. Gibbs and H. A. Gebbie, "Application of Walsh Functions to Transform Spectroscopy," Nature, Vol. 224, 6 December 1969, pp. 1012-1013.

17. J. Pearl, "Effectiveness of Orthogonal Transforms in Information Processing Applications," UCLA-ENG-7387, Final Report, November 1973, AD 771328.

18. J. Bramhall, An Annotated Bibliography on Walsh and Walsh Related Functions, APL/JHU TG 1198B, May 1974.

THE JOHNS HOPKINS UNIVERSITY
APPLIED PHYSICS LABORATORY
SILVER SPRING, MARYLAND

ACKNOWLEDGMENT

The author wishes to thank M. I. Marks and W. H. Zinger for a number of helpful discussions during the course of this work, and M. M. Jesurun for programming the computations.